2013

# Abiotic Degradation of Chlorinated Hydrocarbons (CHCs) with Zero-Valent Magnesium (ZVM) and Zero-Valent Palladium/ Magnesium Bimetallic (Pd/Mg)-Reductant

Fang Yu
*Wright State University*

# ABIOTIC DEGRADATION OF CHLORINATED HYDROCARBONS (CHCs) WITH ZERO-VALENT MAGNESIUM (ZVM) AND ZERO-VALENT PALLADIUM/MAGNESIUM BIMETALLIC (Pd/Mg)-REDUCTANT

A thesis submitted in partial fulfillment of the
requirements for the degree of
Master of Science

By

FANG YU
B.S., Jilin University, 2010

2013
Wright State University

WRIGHT STATE UNIVERSITY

GRADUATE SCHOOL

July 8, 2013

I HEREBY RECOMMEND THAT THE THESIS PREPARED UNDER MY SUPERVISION BY Fang Yu ENTITLED Abiotic Degradation of Chlorinated Hydrocarbons (CHCs) with Zero-Valent Magnesium (ZVM) and Zero-Valent Palladium/Magnesium Bimetallic (Pd/Mg)-Reductant BE ACCEPTED IN PARTIAL FULFILLMENT OF THE REQUIREMENTS FOR THE DEGREE OF Master of Science

Abinash Agrawal, Ph. D.
Thesis Director

David Dominic, Ph. D.
Chair, Department of Earth and Environmental Sciences

Committee on
Final Examination

Abinash Agrawal, Ph.D.

Mark Goltz, Ph.D.

Songlin Cheng, Ph.D.

William Ayres, Ph.D.
Interim Dean, Wright State University Graduate School

## ABSTRACT

Fang Yu. M.S. Department of Earth and Environmental Sciences, Wright State University, 2013. Abiotic Degradation of Chlorinated Hydrocarbons (CHCs) with Zero-Valent Magnesium (ZVM) and Zero-Valent Palladium/Magnesium Bimetallic (Pd/Mg)-Reductant

Chlorinated hydrocarbons (CHCs) in groundwater can be treated by monometallic and bimetallic metal reductants through abiotic degradation. The breakdown of CHC is achieved by gaining electrons from those reductants and removing chlorines from CHC molecules to transform the CHCs into less chlorinated compounds. As a proven technology in groundwater treatment, permeable reactive barriers (PRBs) have been used to passively treat contaminated groundwater, in which granular metals can be used as reactive materials.

This study explored the abiotic degradation of CHCs by zero-valent magnesium (ZVM) and bimetallic palladium/magnesium (Pd/Mg) reductants. Different CHCs (carbon tetrachloride, chloroform, dichloromethane (DCM), 1,2-dichloroethane (1,2-DCA), 1,1,2-trichloroethane (1,1,2-TCA), 1,1,2,2-tetrachloroethane (1,1,2,2-TeCA), 1,2-dichloropropane (1,2-DCP), and 1,2,3-Trichloropropane (1,2,3-TCP) were chosen as target contaminants.

Results showed that even with its high reduction potential, ZVM did not treat CHCs effectively due to corrosion of Mg by water, which formed

Mg $(OH)_2$(s) precipitate on the metal surface and prevented further reaction. Such inhibition can be reduced by lowering pH conditions. However, in the presence of Pd, CHCs were removed at a much faster rate at neutral pH conditions. Hydrocarbons were produced as sole products, which indicated complete degradation of CHCs by Pd/Mg. Recalcitrant CHCs such as DCM, 1, 1,2-TCA, 1,2-DCP and 1,2,3-TCP were found to be effectively degraded by Pd/Mg. No significant effect of Pd loading on CHC degradation was observed, while the degradation was accelerated by increasing the Mg loading.

TABLE OF CONTENTS

page

LIST OF FIGURES

Figure Page

LIST OF TABLES

ACKNOWLEDGEMENTS

Generous academic assistance was kindly provided by Drs. Abinash Agrawal, Songlin Cheng and Mark Goltz. Kelsey Danner provided technical assistance. Research funding was provided from the United States Air Force, Air Force Institute of Technology, Wright-Patterson Air Force Base, Ohio.

# Chapter 1

## I. BACKGROUND

### I.1 CHCs Pollution in Groundwater

Chlorinate hydrocarbons (CHCs) have been used extensively as solvents for decades in agricultural and industrial applications. The strong carbon-chlorine bond gives CHCs high stabilities, which make CHCs difficult to degrade and they tend to persist for a longer time once they enter the environment. Due to leaks and releases from sources, CHCs are among key pollutant groups that most commonly exist in the groundwater. A study conducted by the United States Geological Survey from 1985 to 1995 showed that CHCs, such as carbon tetrachloride (CT), chloroform (CF) and trichloroethylene (TCE), were the most frequently detected contaminants among 60 volatile organic compounds in the groundwater in rural and urban areas (Squillace *et al.* 1999). Because of their high toxicity and carcinogenicity, many CHCs such as CT and CF have been considered as priority pollutants by the United States Environmental Protection Agency (US EPA 1979).

## I.2 Permeable Reactive Barrier (PRB)

As a proven technology, which is designed for *in situ* remediation of groundwater contaminated with CHCs, PRB has been used to passively treat contaminated groundwater. PRBs involve the placement of a permeable barrier downstream of the contaminant source to treat the plume of contaminated groundwater. PRB can remove or degrade the contaminants within the reactive treatment zone and release treated water downstream. The reactive treatment zone of PRBs can be created by injecting/amending a mixture of reactive material and sand into the subsurface. Numerous studies have investigated various reactive reagents/materials that can be used in PRBs. The primary removal methods in PRBs include physical processes such as sorption and precipitation, biological processes such as biodegradation and chemical processes such as chemical reduction or oxidation. In abiotic degradation processes within a PRB, reductive dechlorination of CHCs is often a key degradation reaction.

## I.3 Reductive dechlorination

Reductive dechlorination is a reaction that can reduce/break one or more carbon-chlorine bonds of a CHC and remove it in the form of chloride ion. The mechanism of CHC dechlorination in natural waters is variable and depends strongly on environmental conditions (Tobiszewski and Namieśnik 2012). Main reductive dechlorination pathways of CHCs are hydrogenolysis and dichloroelimination. (Eqs. 1 and 2 below, where RCl represents a CHC)

Hydrogenolysis:

$$RCl + H^+ + 2e^- \rightarrow RH + Cl^- \quad [1]$$

Dichloroelimination:

$$RCCl - CClR + 2e^- \rightarrow RC = CR + 2Cl^- \quad [2]$$

Several different materials have been investigated to accomplish reductive dechlorination and one of the more effective categories of reagents that have been found are zero valent metals. Based on previous studies, metals that are reactive toward CHCs include zero-valent metals (e.g., $Fe^0$, $Zn^0$, $Sn^0$) etc. and bimetallic reductants, such as Fe/Pd, Zn/Pd, Cu/Al.

## I.4 Hydrolysis and Dehydrochlorination

Besides reductive dechlorination, other dechlorination pathways of CHCs include hydrolysis and dehydrochlorination. Hydrolysis is a slow process in natural waters. Generally, it happens when organic molecule reacts with water, resulting in the formation of a new covalent bond with $OH^-$ and the cleavage of the covalent bond with chlorines. The reaction can be represented by the following equation:

$$RCl + H_2O \rightarrow R - OH + Cl^- + H^+ \quad [3]$$

CHCs may also undergo dehydrochlorination in certain conditions. In dehydrochlorination, HCl is eliminated from CHCs, which results in the formation of double or triple carbon bonds and less chlorinated organic compounds:

$$RHCCl - CRH_2 \rightarrow RHC = CHR + HCl \quad [4]$$

## I.5 Mechanism of Reductive Dechlorination by Zero-Valent Metals

The breakdown of carbon-chlorine bonds of CHC molecules in reductive dechlorination requires an electron donor (reductant), such as zero valent metals; in such systems, CHCs are electron acceptors. (See half-reactions shown below as Eq 5 and 6):

$$Fe^0 \rightarrow Fe^{2+} + 2e^- \quad [5]$$

$$RCl + 2H^+ + 2e^- \rightarrow RH + HCl \quad [6]$$

Research has shown that zero-valent metals such as $Fe^0$ and $Zn^0$ can reduce CHCs effectively (Gillham and O' Hannesin 1994; Matheson and Tratnyek 1994; Boronina *et al.* 1995; Agrawal and Tratnyek 1996; Roberts *et al.* 1996). Based on the success of using microscale metals for degradation of CHCs in groundwater, nanoscale metal particles such as iron, were studied and shown to demonstrate higher degradation efficiency due to their larger surface area (Lien and Zhang 1999; 2001). Nanoscale zero valent iron (nZVI) provides more reactive sites due to the larger surface area, thus allowing for faster degradation of contaminants. (U.S. EPA 2008)

## I.6 Role of Palladium in Bimetallic System

A previous study (Cheng *et al*. 1997) explained the role of Pd in the dehalogenation process. As a hydrogenating catalyst, Pd intercalates the molecular hydrogen generated from the reaction, which in turn forms a reducing agent on the Pd/Zero-valent metal interface to degrade the CHCs that are absorbed onto it. Pd/Fe and bimetallic systems have been examined in numerous investigations (Muftikian *et al.* 1995; Cheng and Wu 2000; Korte *et al.* 2000; Clark II *et al.* 2003). The following equations

represent the reactions that are presumed to occur at the interface of Pd/Mg (Graham and Jovanovic 1999):

$$Mg^0 + H_2O + Pd^0 \text{ (catalyst)} \rightarrow Mg(OH)_2 + Pd_2H_2 \text{ (Pd hydride)} \quad [7]$$

$$Pd_2H_2 + R - X \rightarrow R\text{-}H + Pd^0 + H^+ + X^- \quad [8]$$

## I.7 Motivation

Most of the bench-scale research and field applications have been done with granular/microscale zero-valent iron (ZVI). The advantages of applying zero-valent iron are as follows: it has a relatively strong negative redox potential, it is abundant in the earth's crust, and it produces non-toxic byproducts, which makes it ideal for environmental applications. Although ZVI and its related products have had impressive successes in treating CHCs in groundwater, there are some limitations:

i. ZVI does not work well as a reductant at high pH. During the progress of the reaction, the ZVI corrosion in water leads to increase in pH that favors the formation of iron hydroxides, which precipitates on the surface of iron metal and inhibits the reaction (Matheson and Tratnyek 1994).

ii. Iron is often ineffective to degrade numerous recalcitrant CHCs, such as dichloromethane (DCM), 1,2-dichloroethane, 1,2-dichloropropane, 1,2,3trichloropropane (TCP), polychlorinated biphenyls (PCBs), etc. As a possible intermediate during the degradation of CT (Matheson and Tratnyek 1994), the accumulation of DCM may potentially threaten drinking water sources since the maximum concentration limit for DCM is 5 μg/L.

Hence, further investigations are needed to overcome such limitations. As an inexpensive metal that is common, magnesium is also environmentally benign. Compared to iron, magnesium has a greater thermodynamic driving force, which can be expressed by the reduction potential:

$$Mg^0 \rightarrow Mg^{2+} + 2e^- \quad [E^0 = -2.37V] \qquad [9]$$

$$Fe^0 \rightarrow Fe^{2+} + 2e^- \quad [E^0 = -0.44V] \qquad [10]$$

In other words, Zero-Valent Magnesium or ZVM ($Mg^0$) is a much stronger reducing agent than ZVI. Another advantage of $Mg^0$ is that the solubility of $Mg(OH)_2$ is greater than that of $Fe(OH)_2$ at neutral pH. ($pK_{sp}$ $Mg(OH)_2$ = 11.15; $pKs_p$ $Fe(OH)_2$ = 15.1), which may reduce the loss of $Mg^0$ reactivity due to precipitation of hydroxide on the metal surface (Engelmann et *al.*, 2001).

## I.8 Research Objectives

This study explored ZVM and Pd/Mg bimetallic reductant as the reducing agents in the degradation of CHCs. The target contaminants included the following: CT, CF, DCM, 1,2-dichloroethane (1,2-DCA), 1,1,2-trichloroethane (1,1,2-TCA), 1,1,2,2-tetrachloroethane (1,1,2,2-TeCA), 1,2-dichloropropane (1,2-DCP), and 1,2,3-Trichloropropane (1,2,3-TCP). The objectives of this study are to:

i. Evaluate the degradation potential of the recalcitrant CHCs by $Mg^0$ as a CHC reductant. The study examined the reaction kinetics, degradation products and carbon mass balance. The experimental conditions were varied with respect to reactor pH.

ii. Evaluate the degradation potential of the recalcitrant CHCs by the Pd/Mg bimetallic reductant. The study compared the results of $Mg^0$ with bimetallic Pd/Mg in terms of reaction kinetics, degradation products and carbon mass balance at variable Pd and Mg loadings.

## Chapter 2

# II. MATERIALS AND METHOD

## II.1 Experimental design

Bench-scale experiments with ZVM were carried out in 160 mL serum bottles. Mg granules (commercial grade; Alpha Chemicals) were pre-treated with 50 mL of acetate buffer (25 mM, pH 7) and sonicated for 15 mins prior to use in order to remove any oxide layer on the Mg surface. Acetate solution was decanted after sonication. Serum bottle reactors were then filled with 96 mL of 25 mM acetate solution (prepared at various initial pH) and sealed using a PTFE-lined grey butyl rubber stopper and aluminum crimp. In order to create an anaerobic condition in the batch reactor in the beginning, the serum bottles were bubbled with high-purity $N_2$ gas vigorously for 2 mins. The reactors were then equilibrated on a rotary shaker (Glas Col, Terre Haute, IN) by end-over-end mixing for 30 mins at 70 rpm. $H_2$ gas produced in the reactor during the equilibration was vented at the end of equilibration using a needle pierced through the rubber stopper. CHC stock solution was then injected into the reactors. After injection of CHC stock solution, the reactors were agitated vigorously on a vortex mixer (3 times for 20 sec at 10 sec intervals). The batch reactors were mixed continuously on a rotary shaker as before at 70 rpm. Headspace samples from the batch reactors were withdrawn by 50

μL gastight syringe (Hamilton, Reno, NV) and analyzed by gas chromatography (6890 GC and 7890GC, Agilent Technologies, Santa Clara, CA).

Bench-scale degradation experiments of target contaminants with Pd/Mg were conducted similarly to the procedure described earlier with $Mg^0$. Pd/Mg particles were synthesized using a deposition method. In this procedure, Mg granules were treated with 25 mM acetate solution (prepared at pH 7) in a sonicator for 15 mins. $K_2PdCl_6$ salt solution (5.64 mM) was freshly prepared right before use. 10 mL of 25 mM acetate solution were added to the reactor before the addition of $K_2PdCl_6$ salt solution to make sure the Mg granules make completely contacted with $Pd^{4+}$ in solution within the reactor. The Pd metal deposited on the Mg surface via the following reaction:

$$2Mg^0 + \ + PdCl_6^{2-} \rightarrow 2Mg^{2+} + Pd^{4+} + 6Cl^- \qquad [11]$$

Batch reactors were shaken manually 5 times for 30 sec with 30 sec intervals to allow $Pd^{4+}$ in solution to react with $Mg^0$ and deposit $Pd^0$ onto the Mg surface. Serum bottles were filled up to 96 mL with 25 mM acetate solution prepared at pH 7 and sealed, then bubbled with a stream of $N_2$ gas for 2 mins each to deoxygenate the reactors. The remaining steps of the experiment were similar to the procedure already described.

## II.2 Chemicals and analysis

Mg granules (10-40 mesh, 99.8%) and 1,1,2-TCA (98%) were obtained from Alpha chemicals (MO, USA), CT (99%), CF (99.8%), DCM (99.9%) were purchased from Fisher Scientific (PA, USA), 1,1,2,2-TeCA (98%), 1,2,3-TCP (98%), and 1,2-DCP (98%) were purchased from Acros Organics (NJ, USA). 1,2-DCA (99%) and $K_2PdCl_6$

(99%) were purchased from Sigma-Aldrich (MO, USA). All chemicals used in the study were analytical grade.

CHC stock solutions were prepared by adding 20μL of the organic compounds in to a 160mL serum bottle containing 160mL of organic-free Milli-Q water, and sealed with Teflon-lined rubber stopper and aluminum crimp without headspace. The bottle was rotated for at least 48 hr to allow CHC to dissolve completely. The CHC stock solution was extracted from the sealed bottle using a gastight glass syringe through the stopper.

Concentrations of CHCs (expect DCM) and byproducts such as $CH_4$ and $C_2H_6$ within the reactors were measured by extracting headspace sample with a 50μL gas-tight syringe. Headspace samples were analyzed by HP 6890 series GC system with FID and ECD. $CH_4$ and $C_2H_6$ were separated on a capillary column (GS GasPro, 30m x 0.32mm; J&W Scientific), connected to an FID. CHCs were separated on a capillary column (HP-624, 30m x 0.32mm; Agilent Technologies), connected to an ECD, with helium as the carrier gas. The 6890 GC method settings for FID and ECD analytes were as follows: inlet temperature at 200 ℃, FID and ECD temperatures at 250 ℃ and 300 ℃, respectively, and oven temperature was 100 ℃. The make-up gas for the GC was $N_2$ with a flow rate of 45 mL $min^{-1}$ for the FID and 60 mL $min^{-1}$ for the ECD. The flow rate of $H_2$ and air was 40 mL $min^{-1}$ and 450 mL $min^{-1}$, respectively.

Concentration of DCM within the reactors was measured extracting headspace sample with a 50μL gas-tight syringe. Headspace samples of DCM were analyzed by HP 7890 series gas chromatography (GC) system with flame ionization (FID) and electron capture detectors (ECD). DCM was separated on a capillary column (HP-624, 30m x

0.32mm; Agilent Technologies), connected to an ECD, with helium as the carrier gas at constant flow 1.8 mL $min^{-1}$. The 7890 GC method settings for FID and ECD analytes were as follows: inlet temperature at 250 ℃, FID and ECD temperatures at 250 ℃ and 300 ℃, respectively, and oven temperature was 100 ℃. The make-up gas for the GC was $N_2$ with a flow rate of 25 mL $min^{-1}$ for the FID and 60 mL min-$^{1}$ for the ECD. The flow rate of $H_2$ and air was 30 mL $min^{-1}$ and 450 mL min-$^{1}$, respectively.

## II.3 Data Treatment

The peak area values of CHCs and byproducts such as $CH_4$, $C_2H_6$ and $C_3H_8$ from GC analysis were transformed into their respective concentrations in aqueous phase at equilibrium using laboratory calibration curves which were calculated according to a published method (Burris *et al.* 1996) and their dimensionless Henry's constants. ($K'_H$ for CHCs at 25°C given in Table A1).

The concentration of CHC within in the reactors was plotted on a scatter plot chart with concentration on *y*-axis and the corresponding time on *x*-axis. The pseudo first-order degradation rate constant ($k_{obs\text{-}CHC}$; $h^{-1}$) by Pd/Mg was determined from the slope of ln[CHC amount (μmol)] versus time (hour) scatter plots for the first four points usually within a half hour period. In monometallic ZVM degradation, the degradation rate constant was obtained by fitting points within a 3 hour period due to the relatively slow degradation process.

In carbon mass balance calculation, the initial carbon mass was determined as the average carbon masses that calculated from DI water control samples. The carbon mass fraction of each compound was determined by calculating the ratio of the concentration of the compound over the initial carbon mass within the reactor.

# Chapter 3

## III. RESULTS AND DISCUSSION

### III.1 Chlorinated methane degradations by ZVM

Experiments of CHC degradation by ZVM were done at pH 7 using 25mM acetate buffer. Mg granules in the reactors were transformed into fine white precipitate ($Mg(OH)_2$ ) with evolution of $H_2$. pH values measured at the end of the experiments ranged from 10.5 to 11.5, indicating that the reaction was taking place under strongly alkaline conditions.

CT: A pseudo first-order degradation rate constant of 0.09 $h^{-1}$ was obtained from CT degradation by Mg (Fig.3.1.1). Trace amounts of CF (3% of carbon mass) were produced from the breaking down of CT, indicating a sequential dechlorination reaction within the system. The result was consistent with previous studies using Mg ribbon (Boronina *et al.* 1995). Both methane and ethane production was observed. No CF degradation was observed, which indicated that methane may be directly produced from degradation of CT but not from sequential dechlorination. Trace amounts of ethane (3% of carbon mass) were detected. The generation of ethane may come from the coupling of methane on the Mg surface (Lin *et al.* 2002). 86% carbon mass was recovered at the end of 2.5-hr experiment.

CF: CF was removed slowly ($k_{obs}$ = 0.065 $h^{-1}$) by Mg (Fig.3.1.2). No dechlorination byproduct was detected. Small amounts of methane (10% in carbon mass) and ethane (2% in carbon mass) were the only byproducts observed. The amount of total carbon mass fluctuated, which may be due to adsorption. Compare with CT, CF was more difficult to be degraded by Mg.

DCM: There was not much DCM degradation by Mg (Fig.3.1.3). A first-order degradation rate constant of 0.05 $h^{-1}$was obtained. No dechlorinated byproduct was observed. Unlike CT or CF degradation, no methane or ethane was produced from DCM degradation. 78% carbon mass balance was observed at the end of the experiment. It is hard to say if the mass loss was due to degradation or adsorption.

Compared with previous studies that have been done with Fe powder and Zn powder (Feng and Lim 2005), degradation of chlorinated methanes by ZVM is much slower. The precipitation of $Mg(OH)_2$ onto the metal surface, which served as a protective film to reduce further reaction might be the key factor that inhibited the reaction. Based on the degradation rate constants observed from CT, CF and DCM degradations, the rate constant decreased with less chlorinated compounds, consistent with the previous studies that been done with other zero-valent metals. (Matheson and Tratnyek 1994; Johnson *et al.* 1996; Lien and Zhang 1999; Schrick *et al.* 2002; Janda *et al.* 2004; Song and Carraway 2006).

### III.2 Chlorinated ethane degradation by ZVM

1,1,2-TCA: A slow pseudo first-order degradation rate constant ($k_{obs}$ = 0.033 $h^{-1}$) was observed in 1,1,2-TCA degradation by Mg at pH 7 (Fig.3.2.1). There was not much

1,1,2-TCA degradation within 2.5 hrs. As a dechlorination byproduct, 1,1-DCE (6% of carbon mass) was produced from the degradation, indicating that dehydrochlorination was taking place during the reaction. No ethane production and a 100% carbon mass recovery was observed.

1, 2-DCA: There was nearly no removal of 1,2-DCA ($k_{obs}$ = 0.033 $h^{-1}$, Fig. 3.2.2) by Mg within 2.5 hrs. No dechlorinated or any other byroducts were observed. 94% carbon mass balance was observed.

Several studies in chlorinated ethane degradations have been done with ZVI and ZVZ (Arnold and Roberts 1998; Zemb *et al.* 2010). No significant degradation of 1, 2-DCA was observed in both cases. For 1,1,2-TCA degradations, ZVZ caused the reductive β elimination of 1,1,2-TCA and produced VC, while in this study, such reaction wasz not observed with ZVM.

### III.3 Chlorinated propane degradation by ZVM

Both 1,2-DCP ($k_{obs}$ = 0.144 $h^{-1}$) and 1,2,3-TCP ($k_{obs}$ = 0.102 $h^{-1}$) showed slow degradation by Mg (Fig.3.3.2, Fig.3.2.1). No methane or ethane was produced in both cases. 75% carbon mass recovery was obtained from 1,2-DCP degradation, and 90% was observed in 1, 2, 3-TCP degradation. There was no clear evidence to show if the carbon mass loss was due to degradation or other processes such as adsorption or complexion.

Previous investigations on 1,2,3-TCP degradation by granular Fe and Zn (Sarathy *et al.* 2010) showed no significant removal of 1,2,3-TCP by Fe but 1.0 to 2.5 orders of magnitude greater degradation rate constant for Zn than Fe. Therefore, ZVZ is more effective in 1,2,3-TCP degradation than ZVI and ZVM.

Overall, CHC degradation by ZVM at neutral pH conditions was unexpectedly slow. Not much CHC was removed within 2.5 hrs in all cases. The white precipitate and high pH observed during the reaction evidenced that the corrosion of Mg with water highly almost totally inhibited the degradation reaction. As an active metal, Mg has a relatively high reactivity with water and forms $Mg(OH)_2$, which precipitates onto the metal surface and tends to defeat its high reactivity with CHC. Mg would be only effective in CHC degradation if Mg-CHC reaction rates are comparable with Mg-$H_2O$ rates (Li and Klabunde 1998). However, in this study, Mg granules that were studied reacted much too fast with water than with the CHC, which made it not very useful in CHC degradation. Compared with ZVI and ZVZ, ZVM is less effective in degrading CHC at neutral pH condition. Table 3.1 shows the pseudo first-order degradation rate constants of CHC degradation with ZVM.

### III.4 Effect of pH condition on CHC degradation by ZVM

To study the effect of pH condition on CHC degradation by Mg granules, CT and DCM were chosen as the target contaminants. pH condition was varied over the range from 4.5 to 8.0 by using 25mM acetate buffer adjusted to different pH values with 1 N HCl.

For CT degradation with Mg, the pseudo first-order degradation rate constant was increasing with decreasing pH value (Fig.3.4.1). The degradation process went faster under acidic conditions, consistent with previous results that showed degradation rate dependence on pH for CT degradation by micro-scale zero valent iron (Matheson and Tratnyek 1994). It is possible that lower pH values decreased the tendency of $Mg(OH)_2$ to precipitate onto the metal surface, which reduced the inhibition of CT degradation by Mg

caused by $Mg(OH)_2$. A linear relationship (Fig.3.4.1) was obtained between the pseudo first-order degradation rate constant and pH value. Very similar results for the effect of pH on DCM degradation by Mg (Fig.3.4.2) were observed. Pseudo first-order degradation rate constants of CT and DCM by ZVM at different initial pH conditions are summarized in Table 3.2

### III.5 Chlorinated methane degradation by bimetallic Pd/Mg

CHC degradation by bimetallic Pd/Mg was done at pH 7 using 25mM acetate buffer, exactly under the same experimental conditions as for the monometallic Mg experiments. The $K_2PdCl_6$ solution turned from bright red into light brown after mixing with Mg granules which indicated that Pd was displaced by Mg. The mixture turned into a gray color suspension at the end of the experiment. $H_2$ was produced vigorously from the beginning of the experiment and kept building up within the reactor.

CT : Dechlorination of CT by Pd/Mg (Fig.3.5.1) showed a rapid pseudo first-order degradation rate constant ($k_{obs1}$= 146.24 $h^{-1}$). Compared with ZVM ($k_{obs}$= 0.0904 $h^{-1}$), bimetallic Pd/Mg degraded CT much faster. Two partially dechlorinated byproducts, CF and DCM, were observed from the degradation of CT as intermediates. The production of CF and DCM indicated sequential dechlorination was taking place during reduction of CT by Pd/Mg. Substantial amount of methane (57%) and ethane (15%) were detected. Degradation of CF and DCM were also observed in this study. Methane and ethane are the only two end byproducts detected from CT degradation after 2.5 hrs, which indicated complete dechlorination of CT. There may be a direct transformation from CT and CF to methane because the amount of methane produced started to increase before

the degradation of DCM began. The degradation of methane was corresponded by the accumulation of ethane, which may indicate that ethane was generated by methane coupling on the metal surface (Lin *et al.* 2002). According to the carbon mass fraction, poor carbon mass recovery at the end of the experiment (46% of the calculated spiked CT concentration) was observed. Such low carbon mass balance is unlikely caused by sorption to the metal surface, indicating that reductive dechlorination might not be the only reaction going on in the system.

CF: The degradation rate constant (46.202 $h^{-1}$) of CF (Fig.3.5.2) was relatively slower than that of CT (146.24 $h^{-1}$), which is reasonable because less chlorinated compounds are more persistent than highly chlorinated compounds under anaerobic conditions. However, the degradation of CF by Pd/Mg still demonstrated a rapid process, especially when compared with ZVM ($k_{obs}$= 0.065 $h^{-1}$). All of the CF injected was removed completely within 0.2 hrs. Similar to CT degradation, DCM production was observed, which is consistent with the assumption that the degradation of chlorinated methanes by bimetallic Pd/Mg proceeds by sequential substitution of Cl by H. Methane and ethane productions were similar to the results of CT degradation. Again, poor carbon mass recovery (40%) was observed.

DCM: Results of DCM degradation are shown in Fig.3.5.3. Unlike other bimetallic particles such as nano-scale Ni/Fe, which is inefficient in degrading DCM (Feng and Lim 2005), use of bimetallic Pd/Mg resulted in rapid degradation ($k_{obs1}$= 1.163 $hr^{-1}$) of DCM with methane and ethane as the end products. Compared with CT and CF degradation, the process of DCM degradation went slower. This is expected, the lower the degree of chlorination of an organic compound, the slower the degradation rate is

(consistent with the trend obtained from CHC degradations by ZVM). Also, the reaction slowed down toward the end of the experiment, which may be due to the precipitation of $Mg(OH)_2$ onto the metal surface. Unlike degradation of CT and CF, there was much less methane (3%of carbon mass fraction) and ethane (3% of carbon mass fraction) produced. There was no dechlorination byproduct and poor carbon mass recovery (28%) was observed.

Methane: Ethane was the only byproduct detected during methane degradation with Pd/Mg (Fig.3.5.4), consistent with the results from CT, CF and DCM degradation. Such result confirmed that methane was the source of ethane in degradation of chlorinated methanes by Pd/Mg. Poor carbon mass recovery (56%) was observed.

Overall, bimetallic Pd/Mg demonstrated rapid and complete degradation of chlorinated methanes at neutral pH conditions (Table 3.1). The presence of Pd accelerated the degradation of chlorinated methanes. The dechlorination process can be described by a pseudo first-order reaction. Methane and ethane were the only end products. Sequential dechlorination was observed, however, there was also evidence showing that instead of sequential dechlorination, methane was directly produced from highly chlorinated methanes. Similar to degradation by ZVM, the degradation rate order was CT > CF >DCM. This trend also consistent with chlorinated ethene degradation by nano-scale Pd/Fe (Zhang *et al.* 1998) and Pd/Zn (Li and Klabunde, 1998). The fewer chlorine atoms a chlorinated methane contains, the slower the reaction rate. Poor carbon mass balance was observed in all three cases, indicating that reductive dechlorination was not the only degradation pathway within the system.

### III.6 Chlorinated ethane degradation by bimetallic Pd/Mg

1,1,2,2-TeCA: Degradation of 1,1,2,2-TeCA with Pd/Mg is shown in Fig.3.6.1. There is a rapid degradation rate constant ($k_{obs1}$= 13.296 $h^{-1}$) at pH 7 using 25mM acetate buffer. Mg alone resulted in much slower degradation process ($k_{obs1}$= 1.601 $h^{-1}$). A substantial amount of ethane (60% in carbon mass at maximum) was detected during the degradation as the sole end product. There was no direct evidence showing that if ethane was produced directly from 1,1,2,2-TeCA or if it resulted from a sequential dechlorination process. It is possible that any intermediates produced from sequential dechlorination were degraded to ethane by Pd/Mg so fast that they couldn't accumulate to be detected. Ethane degradation was also observed. To confirm the source of ethane production, different initial concentrations of 1,1,2,2-TeCA were injected into the reactors. The result showed that the amount of ethane produced was consistent with the concentration of 1,1,2,2-TeCA input into the reactors. Higher 1,1,2,2-TeCA initial concentration resulted in more ethane produced, indicating that ethane was a real byproduct of 1, 1, 2, 2-TeCA degradation by Pd/Mg. Higher initial concentration of 1,1,2,2-TeCA also resulted in faster degradation rate constants. (15.93$h^{-1}$ compared with 13.3$h^{-1}$). Poor carbon mass recovery (30%) was observed.

1,1,2-TCA: Rapid degradation of 1,1,2-TCA was observed with a first-order rate constant at 4.887 $h^{-1}$ (Fig.3.6.2). Compared with 1,1,2,2-TeCA degradation, 1, 1, 2-TCA degradation was slower, which is consistent with the trend that less chlorinated hydrocarbons are more resistant to anaerobic degradation. Similar with 1,1,2,2-TeCA degradation, no partially dechlorinated byproduct was detected. The only product observed was ethane. Different concentrations of 1,1,2-TCA were studied to confirm the

source of ethane production. Consistent with what was observed during 1,1,2,2-TeCA degradation, there was more ethane production with higher 1,1,2 -TCA input, indicating that ethane was a real product produced from 1, 1, 2-TCA. Ethane degradation and poor carbon mass recovery (32%) were observed.

1, 2-DCA: The first-order degradation rate constant obtained in 1,2-DCA degradation was 1.26 $h^{-1}$ (Fig.3.6.3), which was slower than the degradation rate of 1,1,2-TCA and 1,1,2,2-TeCA. Unlike 1, 1, 2-TCA and 1, 1, 2, 2-TeCA degradation, no ethane production was observed. Different amounts of 1, 2-DCA were studied and there was no ethane produced even with higher initial concentration of 1, 2-DCA. Degradation rate constants were similar between two experiment with different initial concentrations of 1,2-DCA. Poor carbon mass recovery (22%) was observed after 2.5 hrs.

Ethane: Degradation of ethane was observed (Fig. 3.6.4) by Pd/Mg. No byproduct was detected by the analytical method that was being used in this study. Ethane degradation indicated that bimetallic Pd/Mg was responsible for the mass decline of ethane in 1,1,2,2-TeCA and 1,1,2-TCA degradations. 30% carbon mass balance was found at the end of the experiment, which is consistent with the poor carbon recovery in 1,1,2,2-TeCA and 1, 1, 2-TCA degradations.

Based on the results, bimetallic Pd/Mg can rapidly degrade chlorinated ethane at neutral pH (Table 3.1). Similarto chlorinated methane degradation, degradation of chlorinated ethanes can be described by pseudo first-order kinetics. No dechlorinated byproducts or intermediates were observed in any of the 3 chlorinated ethanes. For 1,1,2,2-TeCA and 1,1,2-TCA, ethane was the main byproduct from the degradation. The

degradation rate also followed the trend that highly chlorinated ethanes are degraded faster, consistent with what was observed in chlorinated methane degradation by Pd/Mg. Unlike the more highly chlorinated compounds, degradation of 1, 2-DCA showed little hydrocarbon production. Poor carbon mass balance indicated that dechlorination was not the only degradation mechanism.

### III.7 Chlorinated propane degradation by bimetallic Pd/Mg

1,2,3-TCP: Degradation of 1,2,3-TCP by bimetallic Pd/Mg is shown in Fig.3.7.1. A pseudo first-order rate constant of 0.979 $h^{-1}$ was obtained. No dechlorinated byproduct was observed during the degradation. The only byproduct that has been detected was propane, indicating that dechlorination was taking place during degradation of 1,2,3-TCP. However, there was no clear evidence to indicate if propane was directly produced from 1,2,3-TCP or from sequential dechlorination. Only a trace amount of propane (3% of total carbon mass) was observed during the degradation, indicating reductive dechlorination was not the only reaction. 27% of carbon mass balance was observed at the end of the degradation.

1,2-DCP: A first-order degradation rate constant of 1.312 $h^{-1}$ was obtained from 1,2-DCP degradation with Pd/Mg (Fig.3.7.2). Similar to degradation of 1,2,3-TCP, no dechlorinated byproduct was detected. However, unlike 1,2,3-TCP, degradation of 1,2-DCP did not produce propane, indicating that propane observed in 1,2,3-TCP degradation might directly result from 1,2,3-TCP but not from sequential dechlorination. Poor carbon mass recovery (12%) was observed after 2.5 hrs.

Overall, bimetallic Pd/Mg removed chlorinated propanes effectively at neutral pH conditions (Table 3.1). The degradation process can be described by pseudo first-order kinetic. Similar to chlorinated ethane degradation, no partially dechlorinated byproduct was observed. Propane was produced from 1,2,3-TCP degradation, which might not come from sequential dechlorination, because no propane was detected during 1,2-DCP degradation.

Removal of CHC by bimetallic Pd/Mg was much more effective than that by ZVM. The presence of Pd accelerated chlorinated organic compound degradation by metal reductants at neutral pH. Such results are consistent with previous studies that had been done studying degradation of chlorinated phenols by Pd/Fe and Pd/Mg (Morales *et al.* 2002), PCB degradation by Pd/Mg (Devor *et al.* 2008) and chlorinated ethene degradation by Pd/Fe and Pd/Zn (Zhang *et al.* 1998). The reason might be that $H_2$ that produced from the corrosion of Mg served as the reductant to degrade CHCs with Pd presented in the system which served as the catalyst. Interestingly, for all CHC degradations, much less amount or even no hydrocarbon such as methane, ethane or propane was produced from the degradation of low-chlorinated CHCs (DCM, 1,2-DCA and 1,2-DCP). Poor carbon mass balance was observed in all CHC degradation, which was different from what was observed in PCB and TCE degradation by Pd/Fe (Grittini 1995; Muftikian *et al.* 1995). In both of those studies, almost 100% carbon mass recoveries were observed. However, poor carbon mass was observed in chlorinated phenol degradation by Pd/Mg (Morales *et al.* 2002), indicating that CHC degradation by Pd/Fe and Pd/Mg may be accomplished via different mechanisms. The lack of carbon mass balance in this study may be due to hydrolysis that produces alcohol or acid or

formation of non-chlorinated low molecular weight compounds, which may have significant volatility (Morales *et al.* 2002). The greater ability of Pd/Mg to degrade CHC may be attributed to several reasons: (1) the deposition of Pd created galvanic Pd-Mg cells leading to increased $H_2$ generation; (2) more $H_2$ production which may serve as another reductant; (3) greater surface areas (Li and Klabunde 1998) or (4) collection of $H_2$ onto the metal surface by Pd (Grittini 1995). The lack of partialy dechlorinated byproducts support the conclusion that CHCs are completed dechlorinated by Pd/Mg. Both methane and ethane were degraded by Pd/Mg with low carbon mass balances. The low carbon mass recovery may be probably due to the activation of C-H bond of the alkanes, which involves the cleavage of C-H and forms metal-C intermediate (Crabree 2004; Arndtsen 1995). Several studies have been done investigating the use of transitional metals such as Pd, Pt and Ni on activation of C-H bond as catalysts (Russell 2012; Rostrupnielsen 1993) showed promising activation of C-H bond. However, all of those studies were done under harsh reaction conditions, such as high temperature. Therefore, it is still unclear if the activation of C-H bond was taking place and responsible for the loss of carbon mass. If it was the case, metal-C intermediate could be converted to syn-gas (mixture of CO and $H_2$ with/without $CO_2$) with the presence of $CO_2$ in the system (Rostrupnielsen 1993).

### III.8 Effect of Pd loading on CHC degradations by bimetallic Pd/Mg

To study the effect of Pd loading on DCM degradation, Pd loadings were varied at 0.02, 0.04, 0.06 and 0.1wt% (6.25mg/L, 13.5mg/L, 18.75mg/L and 31.25mg/L) along with 31.25g/L of Mg granules. There was not much difference in the first-order degradation rate constants of DCM degradation except with Pd loading at 0.1 wt%, which

showed a relatively slower rate (Fig. 3.8.1). It may be possible that at 0.1 wt% Pd loading, too much Pd covered the surface of Mg, inhibiting the galvanic reaction between Pd/Mg. However, when Pd loading ranged from 0.02 to 0.06 wt%, degradation rate constants of DCM degradations were nearly the same. Therefore, there was no discernible effect on DCM degradation kinetics at various Pd loadings within the study range.

For 1,2-DCA degradation, similar results were observed. Pd loadings were varied at 0.02 and 0.06 wt% (6.25mg/L and 18.75mg/L) with Mg granules fixed at 31.25g/L. Results showed that there was not a significant difference between the degradation rates (Fig.3.8.1). A pseudo first-order degradation rate constant of 1.384 $h^{-1}$ was obtained with 0.02 wt% of Pd, comparing with 1.378 $h^{-1}$ when Pd loading was increased to 0.06 wt%.

Both DCM and 1,2-DCA experiments showed insignificant effect of Pd loading on the degradation kinetics within the study range. In previous work that had been done by Grittini in PCB degradation by Pd/Fe (Grittini 1995), higher degradation rate constant was observed with higher dose of palladized iron. Therefore, lack of effect of Pd loading in this study may reflect that within the study range, increasing Pd loading did not increase the amount of palladized magnesium.

### III.9 Effect of Mg loading on CHC degradation by bimetallic Pd/Mg

DCM and 1, 2-DCA were selected to investigate the effect of Mg loading on CHC degradations by bimetallic Pd/Mg. The amount of Pd was fixed at 18.75mg/L (0.06 wt% of 3g of Mg), while Mg loadings varied at 15.625 g/L, 31.25 g/L, 46.875 g/L, 62.5 g/L.

For both DCM and 1, 2-DCA degradation, a good linear correlation was observed between the pseudo first-order degradation rate constant and Mg loading (Fig.3.9.1 and Fig.3.9.2). The degradation process was accelerated by increasing Mg loading, indicating that there was a significant effect of Mg loading on CHC degradation. It is possible that CHC degradation kinetics are affected by surface area (Li and Klabunde 1998). Therefore, the degradation rates depend on the specific surface area of Mg.

# Chapter 4

## IV. CONCLUSIONS

This study investigated the degradation kinetics of CHCs by ZVM and bimetallic Pd/Mg, abiotic reductants. Even though ZVM has a relative higher reduction potential compared with iron and zinc, its fast reaction with water inhibit its effectiveness in degrading CHCs. The formation and precipitation of $Mg(OH)_2$ highly reduce its ability to degrade CHC, resulting in slower degradation kinetic compared with ZVI and ZVZ. However, under acidic conditions which reduce the tendency of $Mg(OH)_2$ to precipitate can accelerate CHC degradation (Table 3.2).

Compared with ZVM, bimetallic Pd/Mg demonstrated much more effectiveness in CHC removal at neutral pH conditions (Table 3.1). Recalcitrant CHCs such as DCM, 1, 2-DCA and 1, 2, 3-TCP were successfully degraded by Pd/Mg. Production of hydrocarbons from CHC degradation indicated complete degradation of CHC with Pd/Mg. Similarly to what was found for other metal reductants, highly chlorinated CHCs are degraded faster in the presence of Pd/Mg to lower chlorinated CHCs. Both reductive dechlorination and hydrolysis may happen in CHC degradation with Pd/Mg. There was not a significant effect of Pd loading on CHC degradation within the study range; however, the degradation kinetics did depend on Mg loading.

As a coarse material that could be filled in PRBs as a reactive reagent, ZVM is not a good choice due to its ineffectiveness in treating CHCs; however, Pd/Mg granule might be a good candidate, especially in dealing with recalcitrant CHCs.

## V. REFERENCES


Agrawal, A.; Tratnyek P.G. Reduction of nitro aromatic compounds by zero-valent iron metal. *Environ. Sci. Technol.* **1996**, *30*, 153—160.

Arndtsen, B.A.; Bergman, R.G.; Mobley, T.A.; Peterson, T.H. Selective intermolecular carbon–hydrogen bond activation by synthetic metal complexes in homogeneous solution. *Acc. Chem. Res.* **1995,** *28* (3), 154—162.

Arnold, W.A.; Roberts, A.L. Pathways and kinetics of chlorinated ethylene and chlorinated acetylene reaction with Zn(0). *Environ. Sci. Technol.* **1998**, *33*, 1956—1956.

Boronina, T.; Klabunde, K. J.; Sergeev, G. Destruction of organohalides in water using metal particles: carbon tetrachloride/water reactions with magnesium, tin, and zinc. *Environ. Sci. Technol.* **1995**, *29*, 1511—1517.

Burris, D. R.; Delcomyn, C. A.; Smith, M. H.; Roberts, A. L. Reductive dechlorination of tetrachloroethylene and trichloroethylene catalyzed by vatamin B-12 in homogenous and heterogeneous systems. *Environ. Sci. Technol.* **1996**, *30*, 3047—3052.

Cheng, I. F.; Fernando, Q.; Korte, N. Electrochemical dechlorination of 4-chlorophenol to phenol *Environ. Sci. Technol.* **1997**, *31*, 1074—1078.

Cheng, S. F.; Wu, S. C. The enhancement methods for the degradation of TCE by zero-valent metals. *Chemosphere* **2000**, *41*, 1263—1270.

Clark II, C.J.; Rao, P.S.C.; Annable, M.D. Degradation of perchloroethylene in cosolvent solution by zero-valent iron. *J. Hazard. Mater.* **2003,** 65—78.

Crabree, R.H. Organometallic alkane CH activation. *J. Organometal. Chem.* **2004,** *689,* 4083—4091.

Devor, R.; Carvalho-Knighton, K.; Aitken, B.; Maloney, P.; Holland, E.; Talalaj, L; Fidler, R.; Elsheimer, S.; Clausen, C.A.; Geiger, C.L. Dechlorination comparsion of mono-substituted PCBs with Mg/Pd in different solvent systems. *Chemosphere* **2008**, *73,* 896—900.

Engelmann, M. D.; Doyle, J. G.; Cheng, F. The complete dechlorination of DDT by magnesium/Palladium bimetallic particles. *Chemosphere* **2001**, *43,* 195—198.

Feng, J.; Lim, TT. Pathways and kinetics of carbon tetrachloride and chloroform reductions by nano-scale Fe and Fe/Ni particles: comparison with commercial micro-scale Fe and Zn. *Chemosphere* **2004**, *59,* 1267—1277.

Gillham, R. W.; O'Hannesin, S.F. Enhanced degradation of halogenated aliphatics by zero-valent iron. *Groundwater* **1994**, *32* (6), 958—967.

Graham, L. J.; Jovanovic, G. Dechlorination of p-chlorophenol on a Pd/Fe catalyst in a magnetically stabilized fluidized bed; Implications for sludge and liquid remediation, *Chemical Engineering* **1999**, *54*, 3085—3093.

Grittini, C.; Fernando, Q.; Korte, N. Rapid dechlorination of polychlorinated biphenyls on the surface of a Pd/Fe bimetallic system. *Environ. Sci. Technol.* **1995**, *29*, 2898—2900.

Janda, V.; Vasek, P.; Bizova, J.; Belohlav, Z. Kinetics models for volatile chlorinated hydrocarbons removal by zero-valent iron. *Chemosphere* **2004**, *54,* 917—925.

Johnson, T.L.; Scherer, M.M.; Tratnyek, P.G. Kinetiacs of halogenated organic compound degradation by iron metal. *Environ. Sci. Technol.* **1996**, *30*, 2634—2640.

Korte, N. E.; Zutman, J. L.; Schlosser, R.M.; Liang, L.; Gu, B.; Fernando, Q. Field application of palladized iron for the dechlorination of trichloroethene. *Waster Manage* **2000,** 687—694.

Li, W.F.; Klabunde, K.J. Ultrafine zinc and nickel, palladium, silver coated zinc particles used for reductive dehalogenation of chlorinated ethylenes in aqueous solution. *Croat. Chem. Acta* **1998,** *71,* 853—872.

Lien, H. L.; Zhang, W. Transformation of chlorinated methanes by nanoscale particles. *Journal of Environmental Engineering* **1999**, *125*, 1042—1047.

Lien, H. L.; Zhang, W. Nanoscale particles for complete reduction of chlorinated ethenes. *Colloids and Surfaces A: Physicochemical and Engineering Aspects* **2001**, *191,* 97—106.

Lin, Y.Z.; SUN, J.; Yi, J.; Lin, J.D.; Cheng, H.B.; Liao, D.W. Energetics of chemisorption and conversion of methane on transition metal surface. *J. Mol. Struct. Theochem.* **2002,** *587,* 63—71.

Matheson, L. J.; Tratnyek, P. G. Reductive dehalogenation of chlorinated methanes by iron metal. *Environ. Sci. Technol.* **1994**, *28*, 2045—2053.

Morales, J.; Hutcheson, R.; Cheng, F. Dechlorination of chlorinated phenols by catalyzed and uncatalyzed Fe(0) and Mg(0) particles. *J. Hazard. Mater.* **2002,** *B90,* 97—108.

Muftikian, R.; Fernando, Q.; Korte, N. A method for the rapid dechlorination of low molecular weight chlorinated hydrocarbons in water. *Wat. Res.* **1995,** 2434—2439.

Roberts, A. L.; Totten, L. A.; Arnold, W. A.; Burris, D. R.; Campbell, T. J. Reductive elimination of chlorinated ethylenes by zero-valent metals. *Environ. Sci. Technol.* **1996**, *30* (8), 2434—2439.

Rostrupnielsen, J.R.; Hansen, J.H.B. $CO_2$-reforming of methane over transition-metals. *J. Catal.* **1993,** *144* (1), 38—49.

Russell, J.; Zapol, P.; Kral, P.; Curtiss, L.A. Methane bond activation by Pt and Pd subnanometer clusters supported on graphene and carbon nanotubes. *Chem. Phys. Lett.* **2012,** 536, 9—13.

Sarathy, V.; Salter, A.J.; Nurmi, J.T.; Johnson, G.O.; Johnson, R.L.; Tratnyek, P.G. Degradation of 1,2,3-Trichloropropane (1,2,3-TCP): Hydrolysis, elimination, and reduction by iron and zinc. *Environ. Sci. Technol.* **2010**, *44*, 787—793.

Schrick, B.; Blough, J.L.; Jones, A.D.; Mallouk, T.E. Hydrodechlorination of trichloroethylene to hydrocarbons using bimetallic nickel-iron nanoparticles. *Chem. Mater.* **2002,** *14*, 5140—5147.

Song, H.; Carraway, E.R. Reduction of chlorinated methanes by nano-sized zero-valent iron. Kinetics, pathways, and effect of reaction conditions. *Environ. Eng. Sci.* **2006,** *23*, 272—284.

Squillace, P. J.; Moran, M. J.; Lapham, W. W.; Price, C. V.; Clawges, R. M.; Zogorski, J. S. Volatile organic compounds in untreated ambient groundwater of the United States, 1985—1995. *Environ. Sci. Technol.* **1999,** *33*, 4176—4187.

Tobiszewski, M.; Namieśnik, J. Abiotic degradation of chlorinated ethanes and ethenes in water. *Environ. Sci. Pollut. Res.* **2012,** *19,* 1994—2006.

U.S. EPA. *Water-related environmental fate of 129 priority pollutants*; EPA-440/4-79-029B; Vol. II: Halogenated aliphatic hydrocarbons, halogenated ethers, monocyclic aromatics, phthalate esters, polycyclic aromatic hydrocarbons, nitrosamines, and miscellaneous compounds. Office of Water Planning and Standards: Washington, DC, **1979**.

U.S. EPA. *Nanotechnology: Practical considerations for use in groundwater remediation;* Office of superfund, remediation and technology innovation: National Association of Remedial Project Managers Annual Training Conference, Portland, Oregon, **2008**.

Zemb, O.; Lee, M.; Low, A.; Manefield, M. Reactive iron barriers: a niche enabling microbial dehalorespiration of 1,2-dichloroethane. *Appl. Microbiol. Biotechnol.* **2010,** *88,* 272—284.

Zhang, W.X.; Wang, C.B.; Lien, H.L. Treatment of chlorinated organic contaminants with nanoscale bimetallic particles. *Catal. Today* **1998,** *40(4),* 387—395.

+

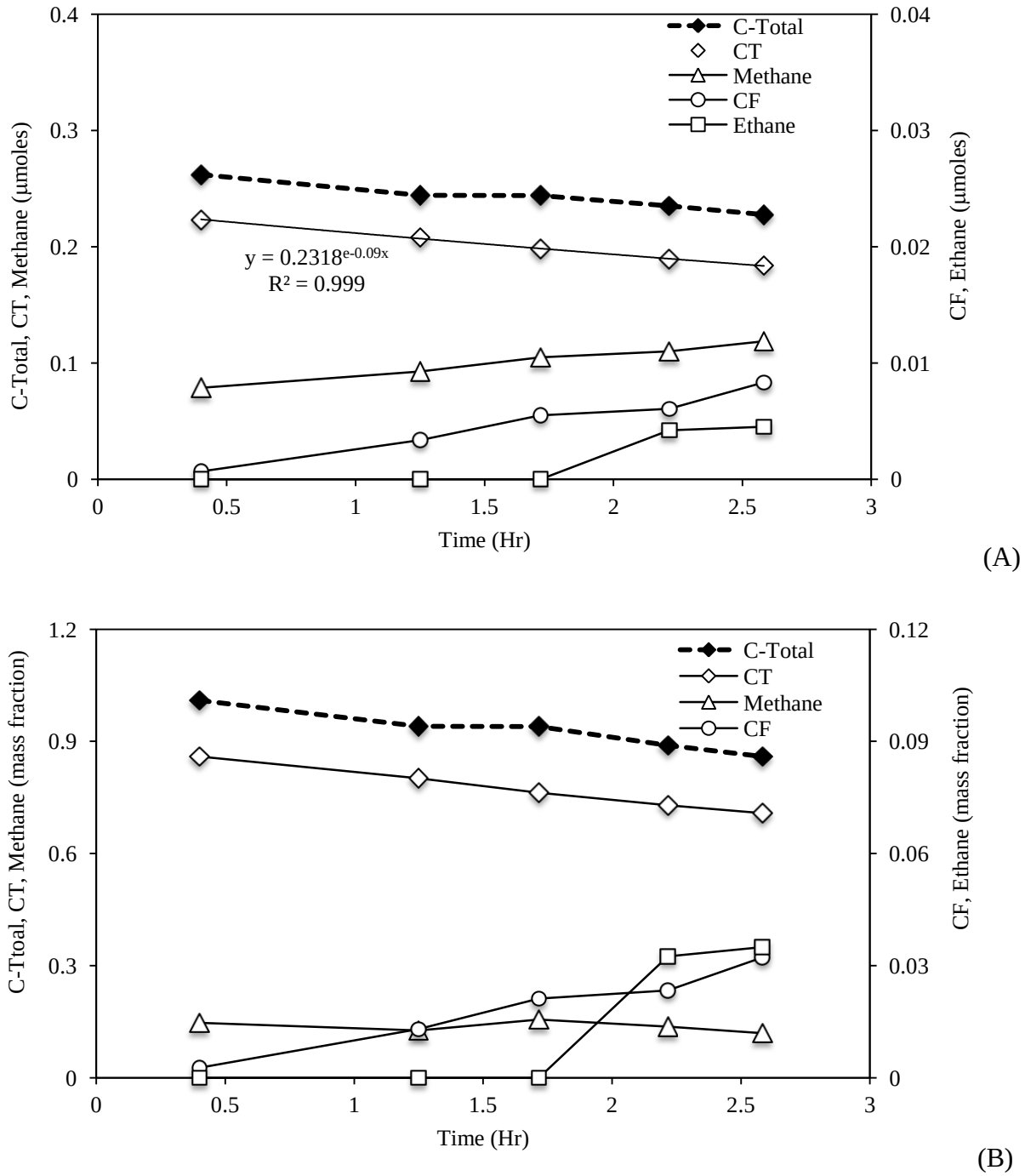


**Figure 3.1.1** CT degradation with 3g Mg at pH 7. $[CT]_0$ = 2.67 mM (200µl 197.5 mg/L CT stock solution). (A) Degradation kinetics; (B) Carbon mass recovery

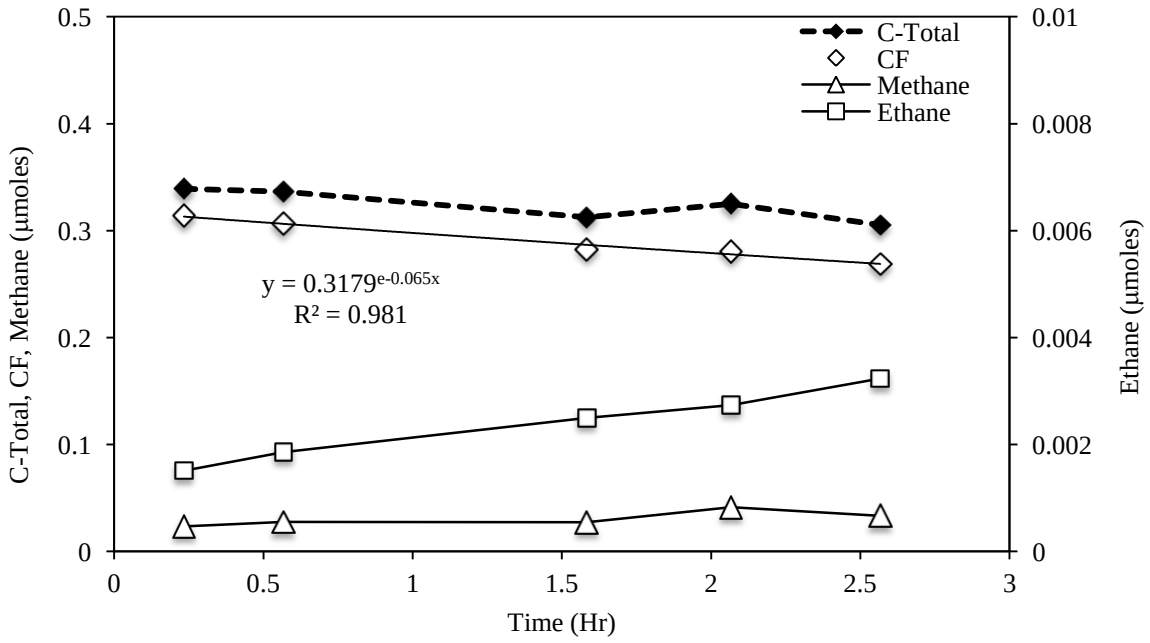


(A)

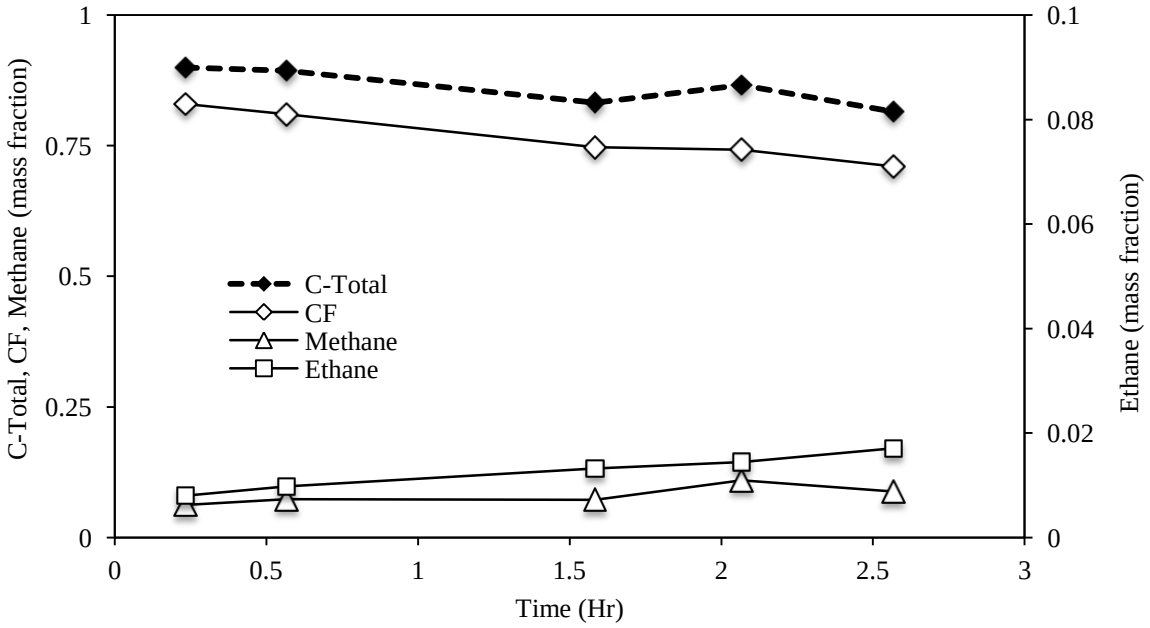


(B)

**Figure 3.1.2** CF degradation with 3g Mg at pH 7. $[CF]_0$ = 3.23 mM (200µl 185 mg/L CF stock solution). (A) Degradation kinetics; (B) Carbon mass recovery

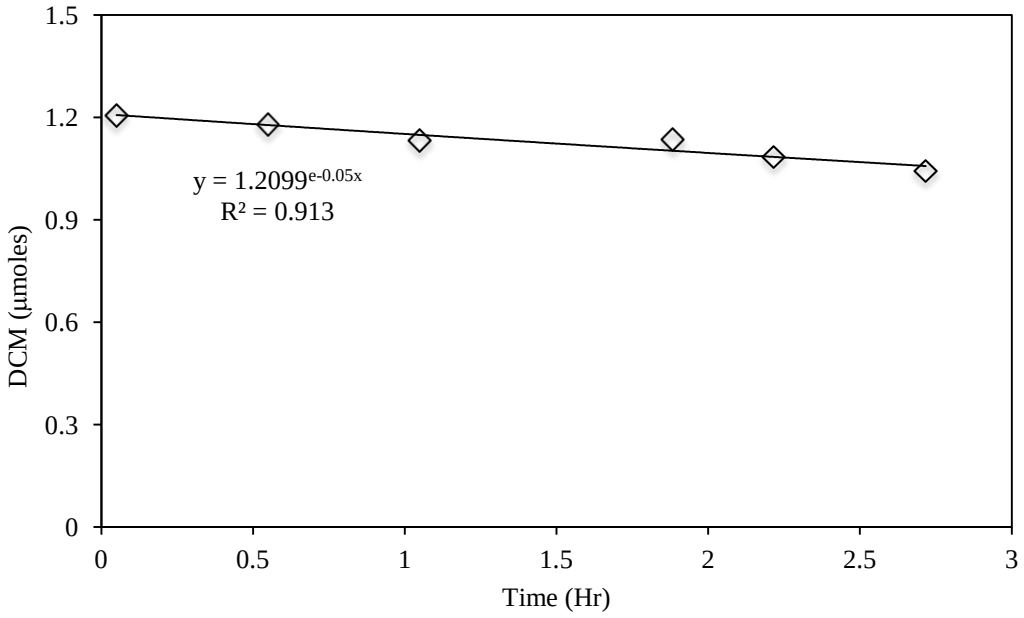


(A)

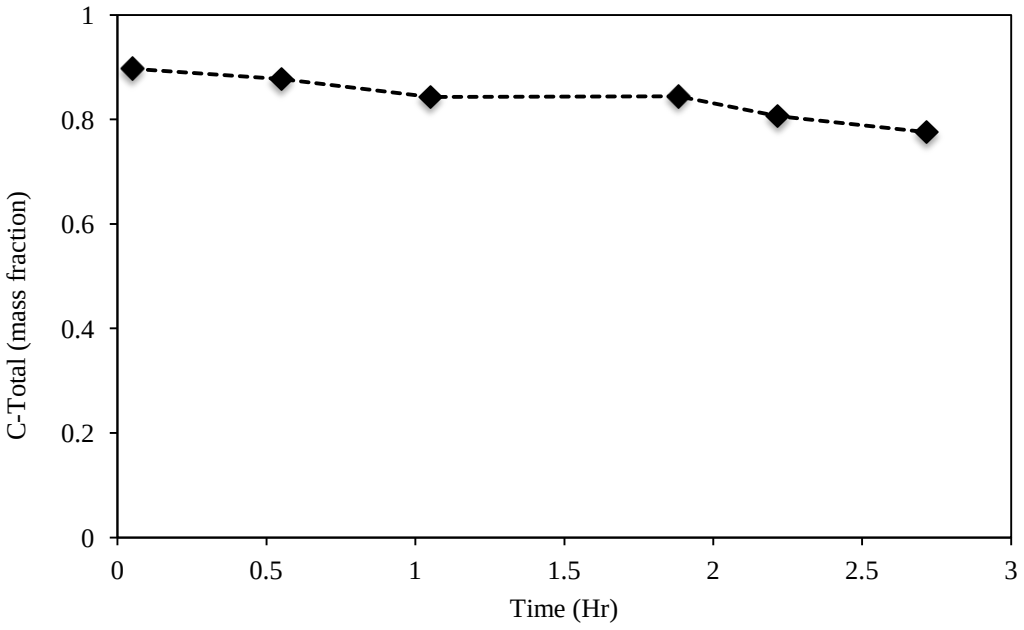


(B)

**Figure 3.1.3** DCM degradation with 3g Mg at pH 7. $[DCM]_0$ = 10.20 mM (500µl 186.3 mg/L DCM stock solution). (A) Degradation kinetics; (B) Carbon mass recovery

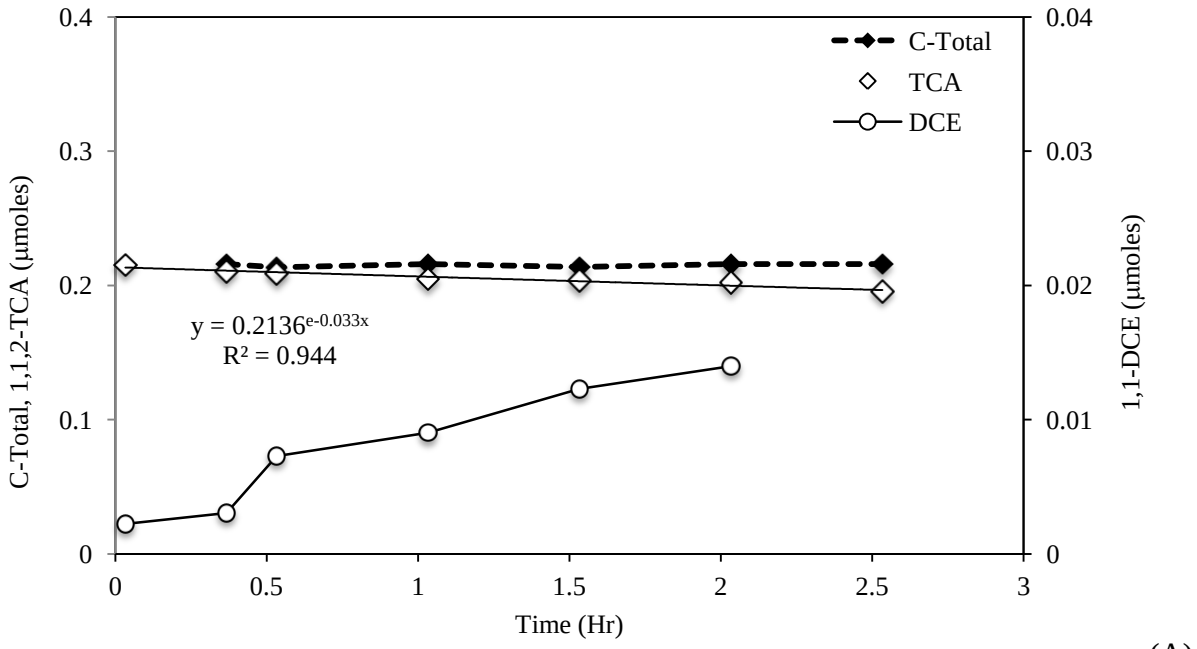


(A)

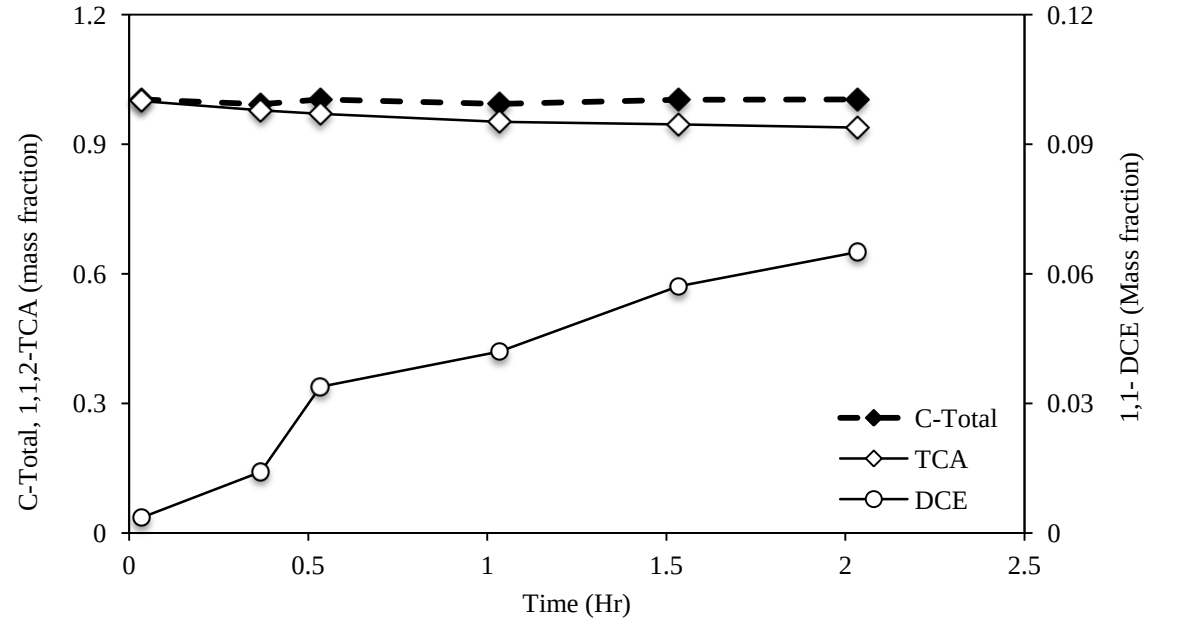


(B)

**Figure 3.2.1** 1,1,2-TCA degradation with 3g Mg at pH 7. $[1,1,2\text{-TCA}]_0$ = 2.80 mM (200µl 179.38 mg/L 1,1,2-TCA stock solution). (A) Degradation kinetics; (B) Carbon mass recovery

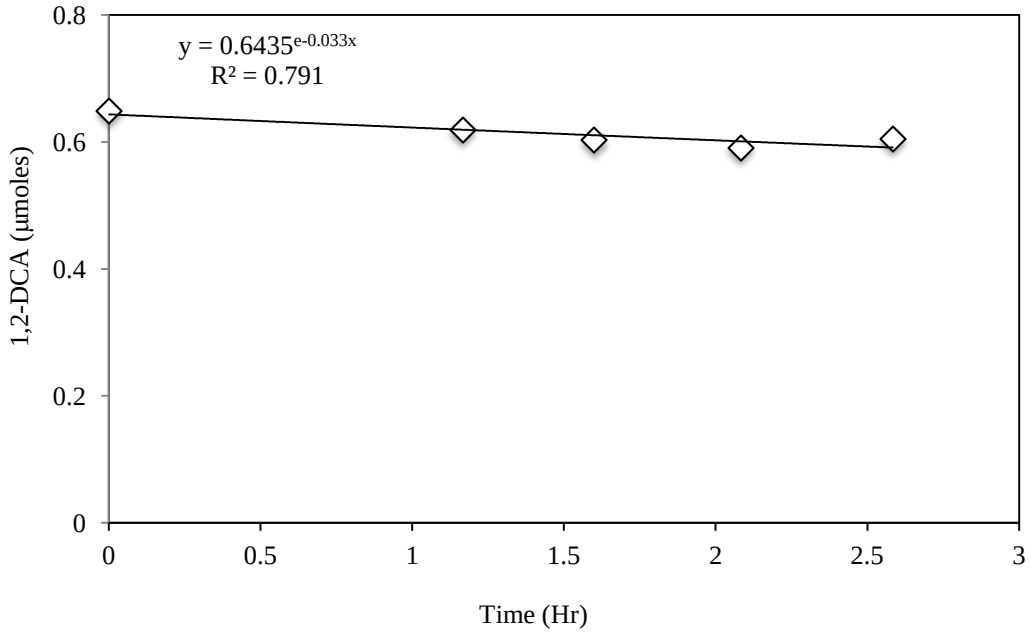


(A)

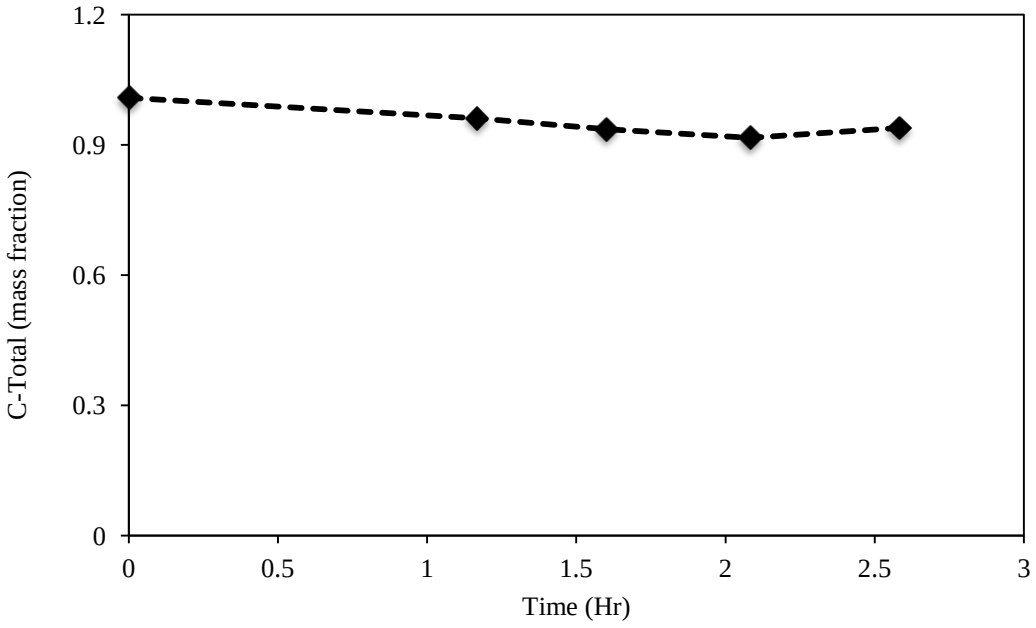


(B)

**Figure 3.2.2** 1,2-DCA degradation with 3g Mg at pH 7. $[1,2\text{-DCA}]_0$ = 3.29 mM (200µl 156.63 mg/L 1,2-DCA stock solution). (A) Degradation kinetics; (B) Carbon mass recovery

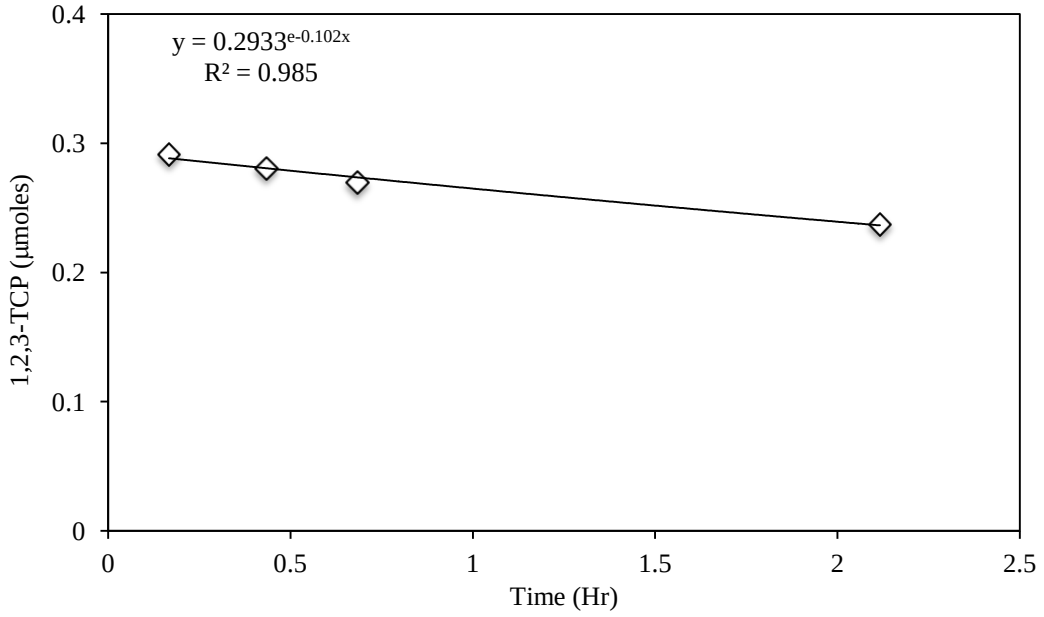


(A)

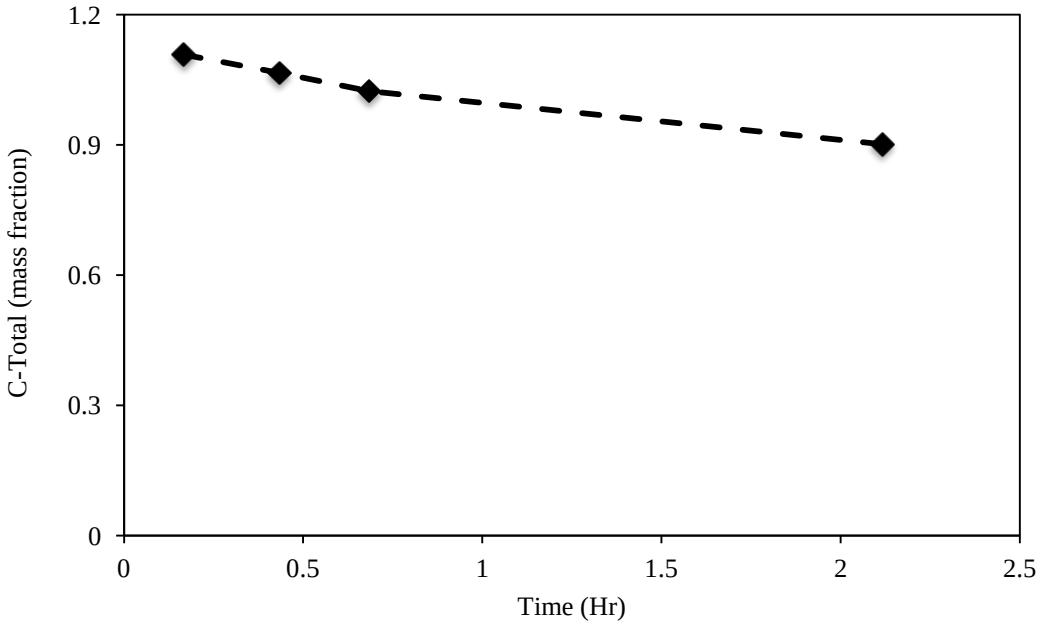


(B)

**Figure 3.3.1** 1,2,3-TCP degradation with 3g Mg at pH 7. $[1,2,3\text{-TCP}]_0$ = 2.44 mM (200µl 172.5 mg/L 1,2,3-TCP stock solution). (A) Degradation kinetics; (B) Carbon mass recovery

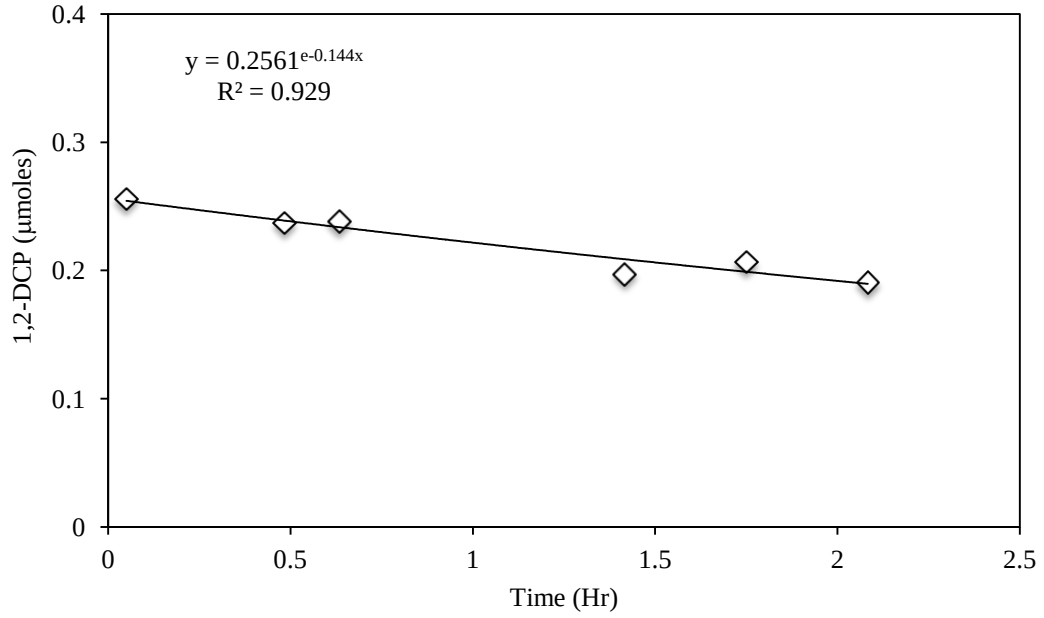


(A)

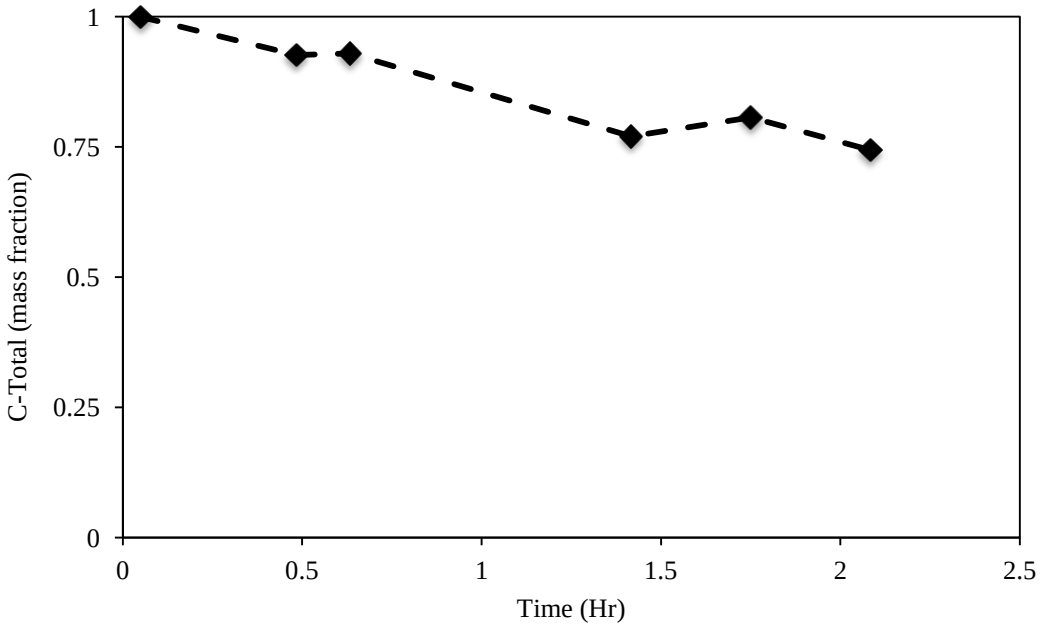


(B)

**Figure 3.3.2** 1,2-DCP degradation with 3g Mg at pH 7. $[1,2\text{-DCP}]_0$ = 2.67 mM (200µl 144.5 mg/L 1,2-DCP stock solution). (A) Degradation kinetics; (B) Carbon mass recovery

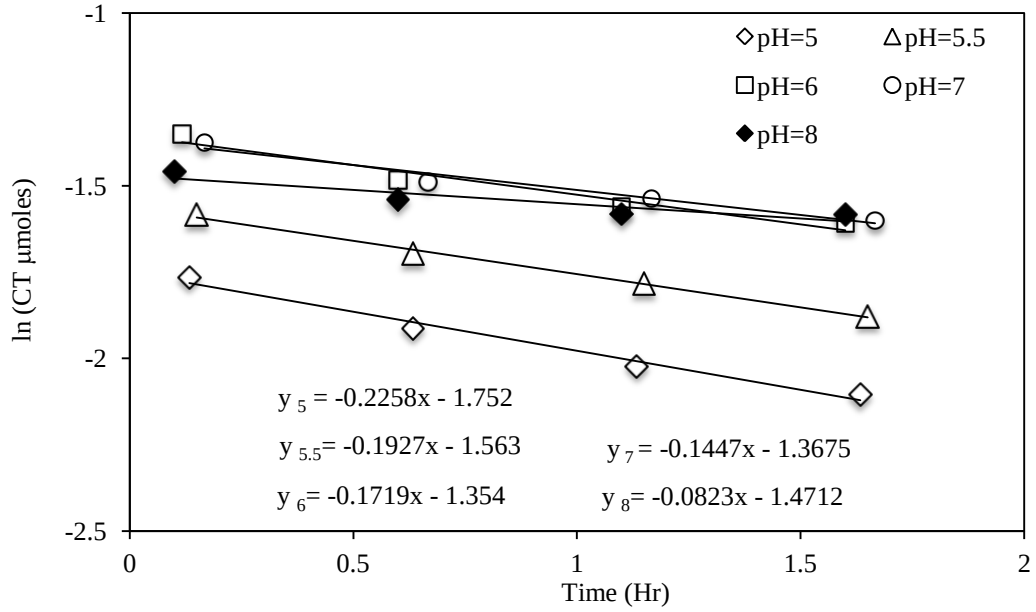


(A)

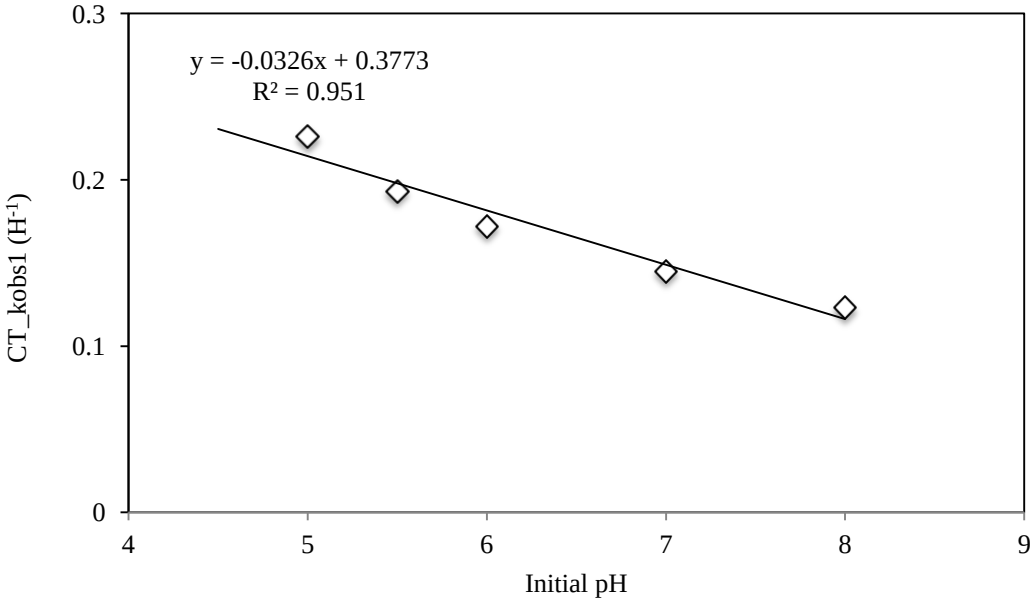


(B)

**Figure 3.4.1** CT degradation with 3g Mg at different initial pH. $[CT]_0$ = 2.27 mM (200µl 197.5 mg/L CT stock solution). (A) Degradation kinetics; (B) Relationship between initial degradation rate constant ($k_{obs1}$, $H^{-1}$) and initial pH

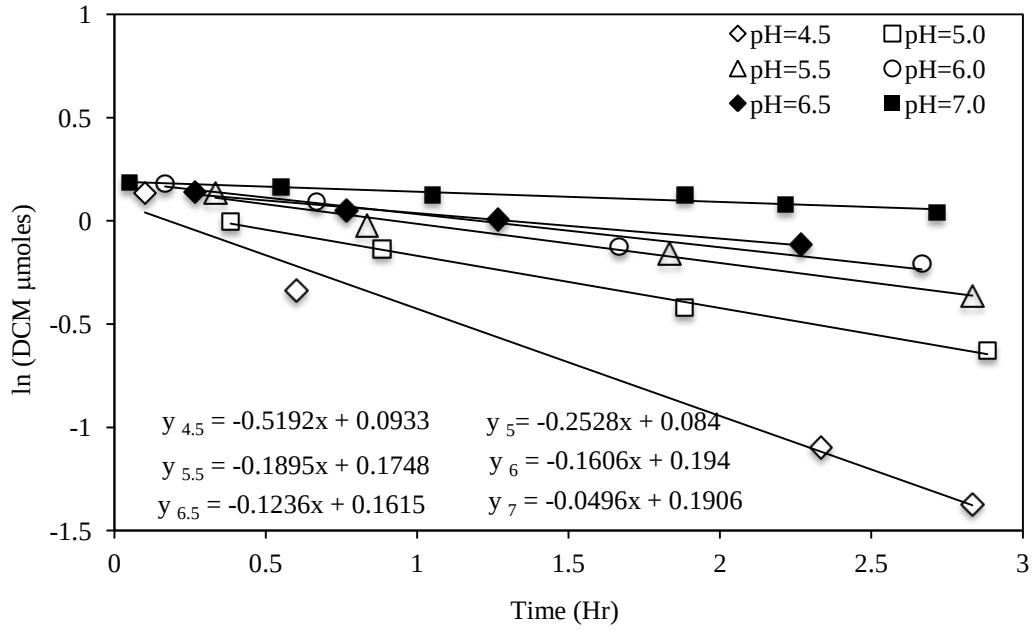


(A)

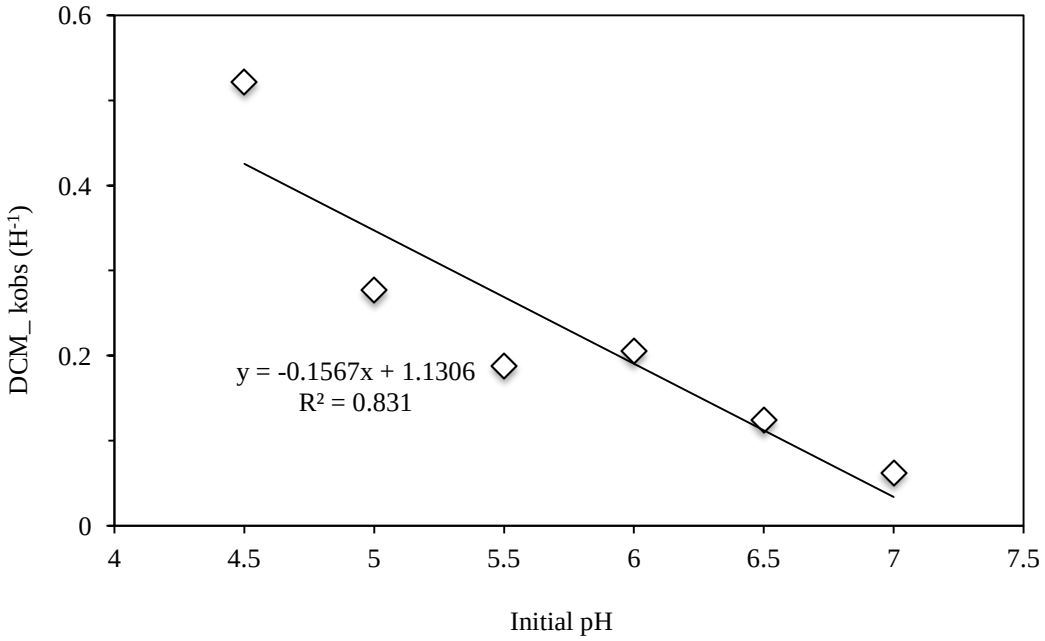


(B)

**Figure 3.4.2** DCM degradation with 3g Mg at different initial pH. $[DCM]_0$ = 10.20 mM (500µl 186.3 mg/L DCM stock solution). (A) Degradation kinetics; (B) Relationship between initial degradation rate constant ($k_{obs1}$, $H^{-1}$) and initial pH

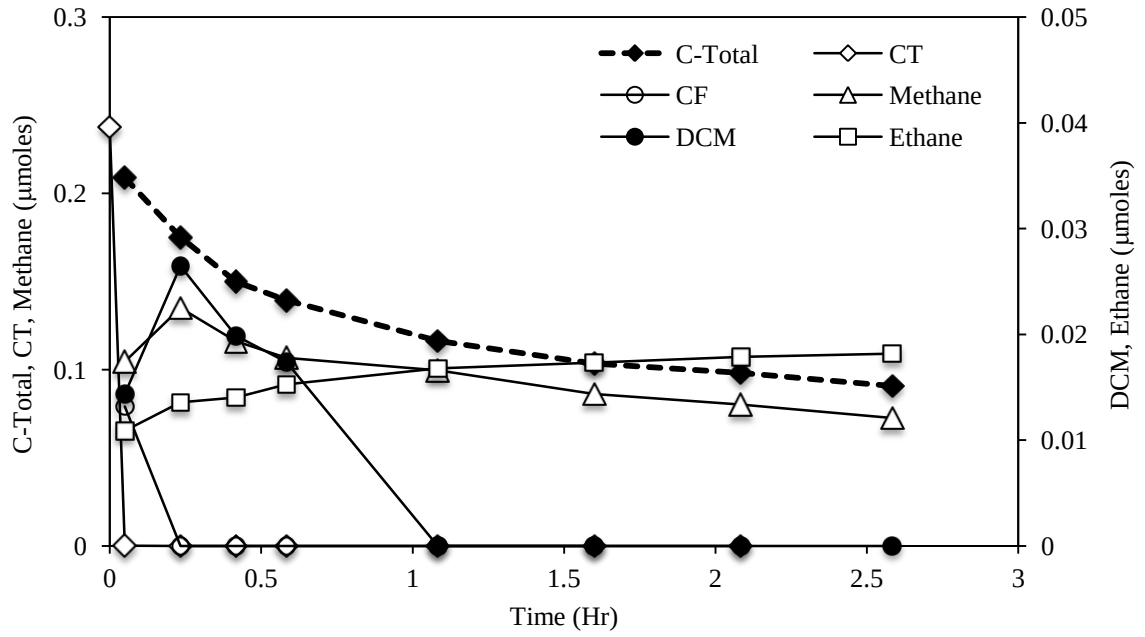


(A)

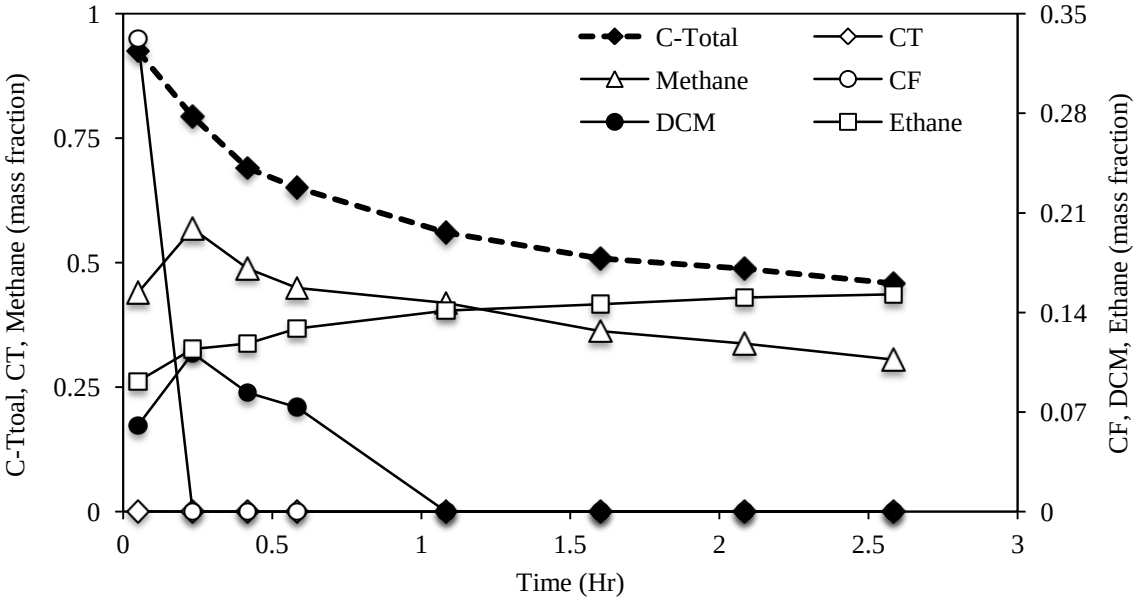


(B)

**Figure 3.5.1.a** CT degradation with Pd/Mg (3 g Mg with 0.06 wt% Pd) at pH 7. $[CT]_0$ = 2.67 mM (200µl 197.5 mg/L CT stock solution). (A) Degradation and byproducts; (B) Carbon mass recovery

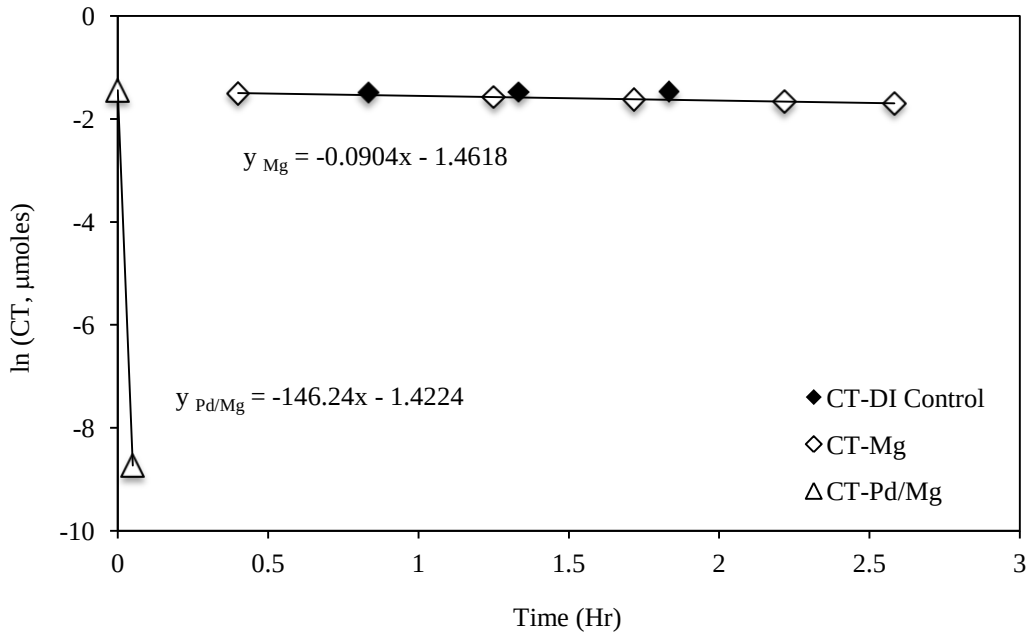


**Figure 3.5.1.b** Degradation kinetics of CT degradation with Pd/Mg (3 g Mg with 0.06 wt% Pd) at pH 7. $[CT]_0$ = 2.67 mM (200µl 197.5 mg/L CT stock solution).

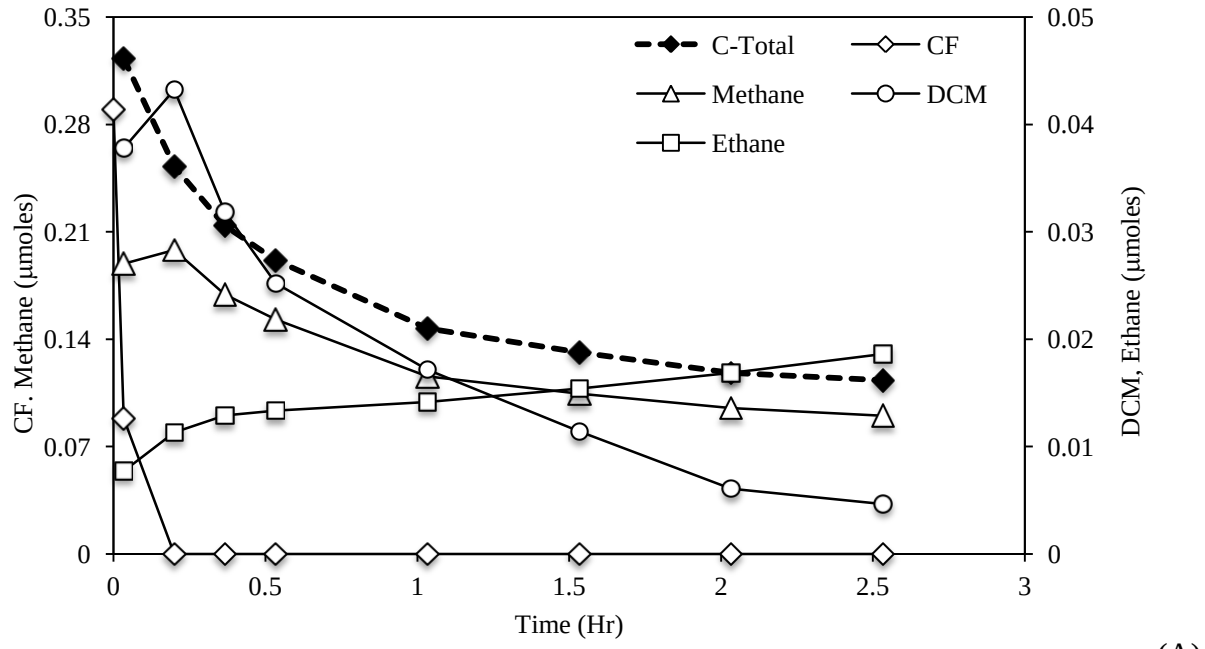


(A)

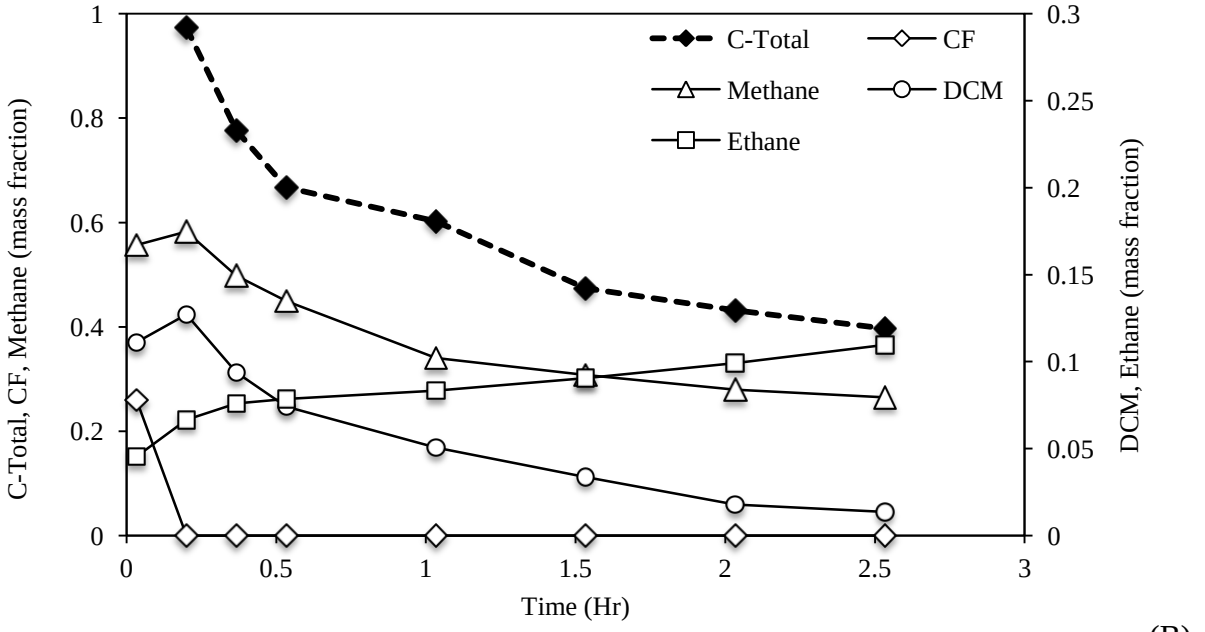


(B)

**Figure 3.5.2.a** CF degradation with Pd/Mg (3 g Mg with 0.06 wt% Pd) at pH 7. $[CF]_0$ = 3.23 mM (200µl 185 mg/L CF stock solution). (A) Degradation and byproducts; (B) Carbon mass recovery

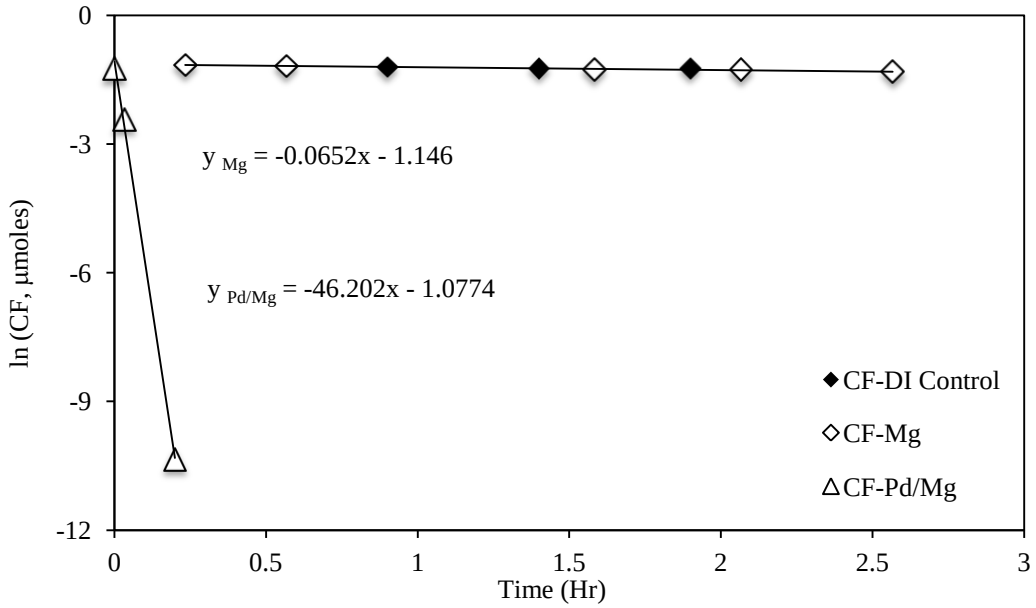


**Figure 3.5.2.b** Degradation kinetics of CF degradation with Pd/Mg (3 g Mg with 0.06 wt% Pd) at pH 7. $[CF]_0$ = 3.23 mM (200µl 185 mg/L CF stock solution).

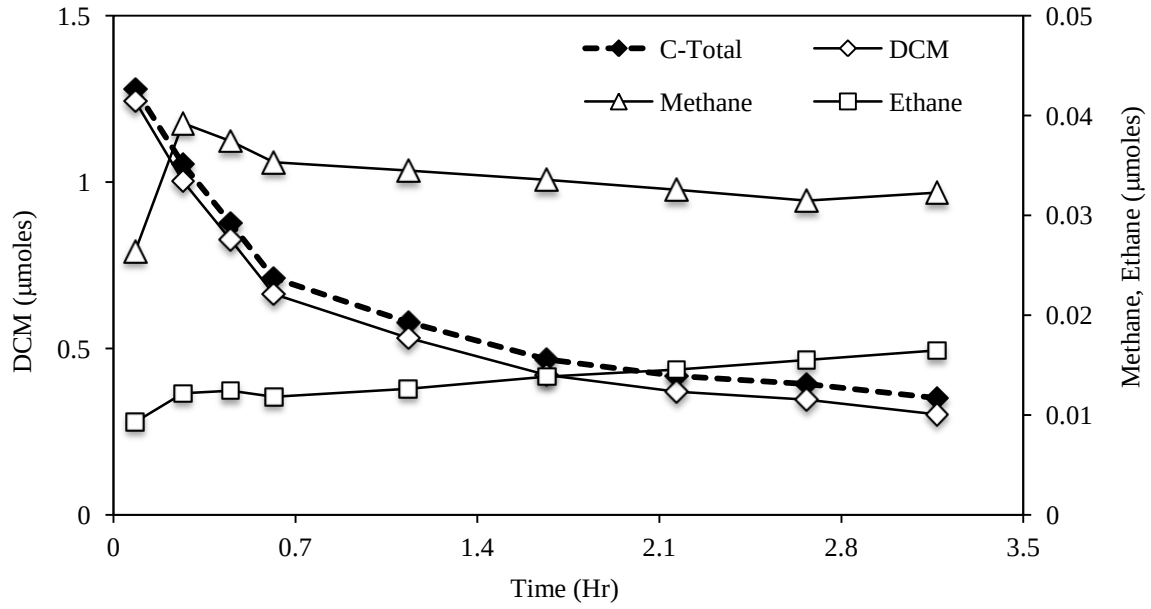


(A)

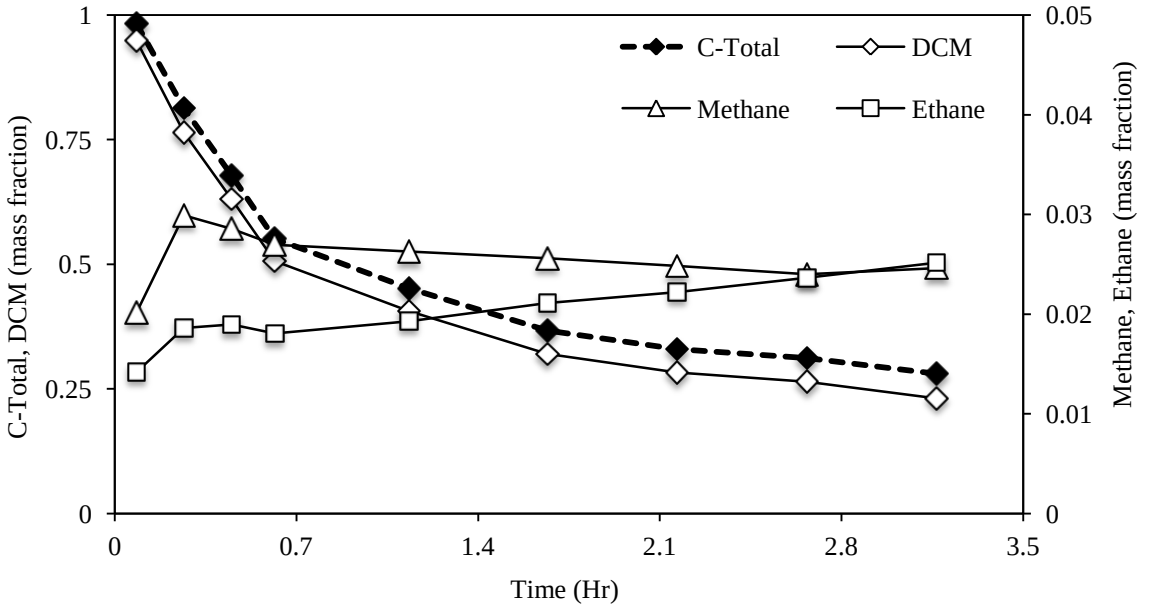


(B)

**Figure 3.5.3.a** DCM degradation with Pd/Mg (3 g Mg with 0.06 wt% Pd) at pH 7. $[DCM]_0$ = 10.20 mM (500µl 186.3 mg/L DCM stock solution). (A) Degradation and byproducts; (B) Carbon mass recovery

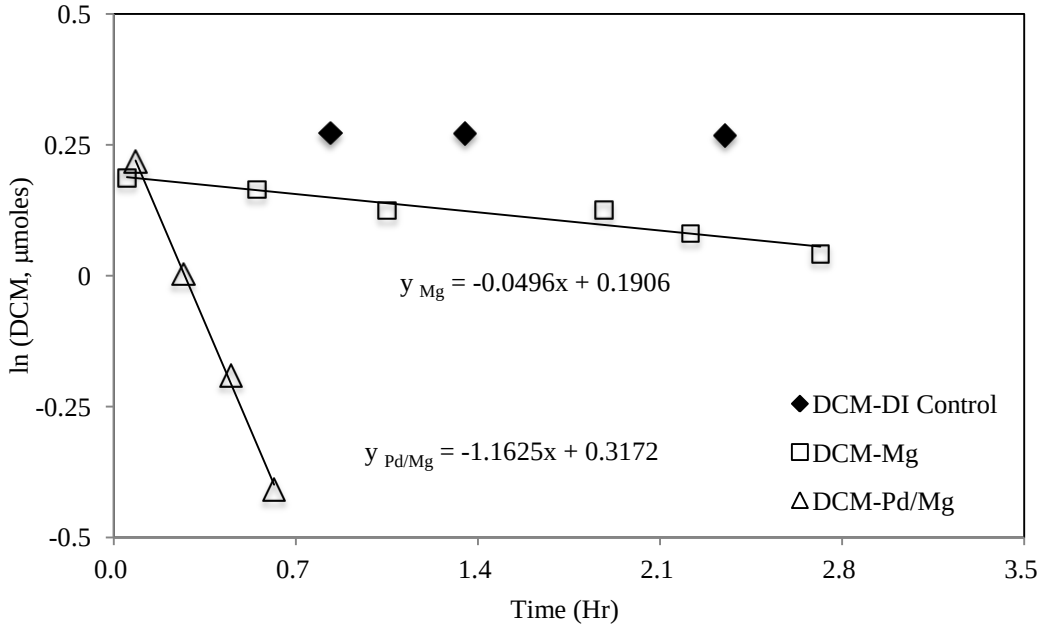


**Figure 3.5.3.b** Degradation kinetics of DCM degradation with Pd/Mg (3 g Mg with 0.06 wt% Pd) at pH 7. $[DCM]_0$ = 10.20 mM (500µl 186.3 mg/L DCM stock solution).

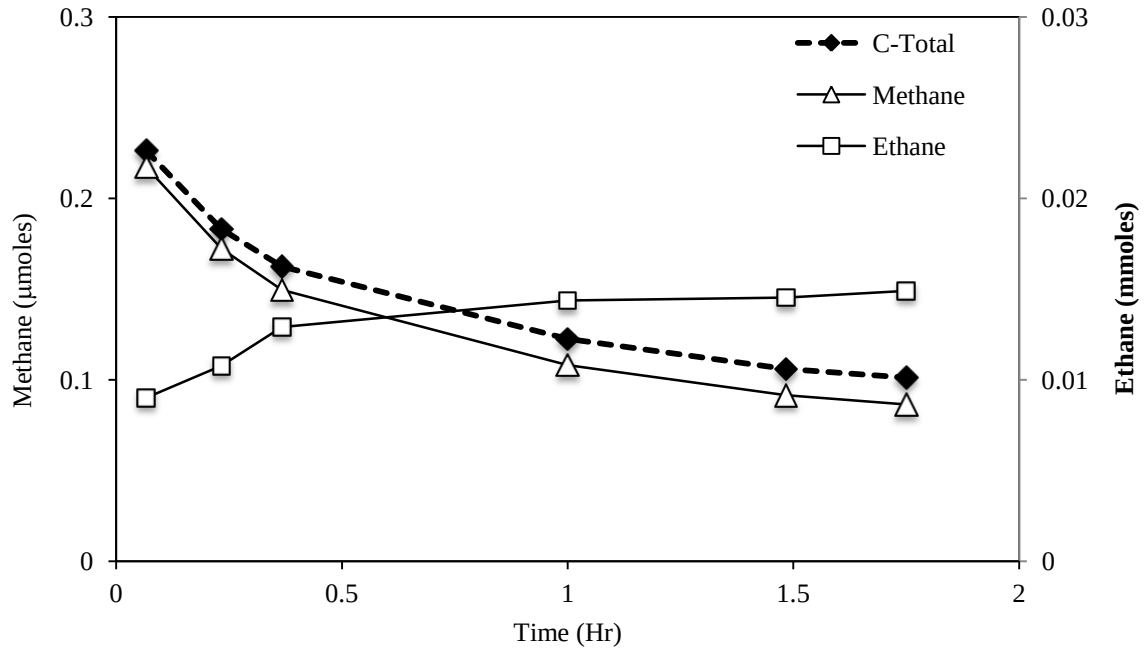


(A)

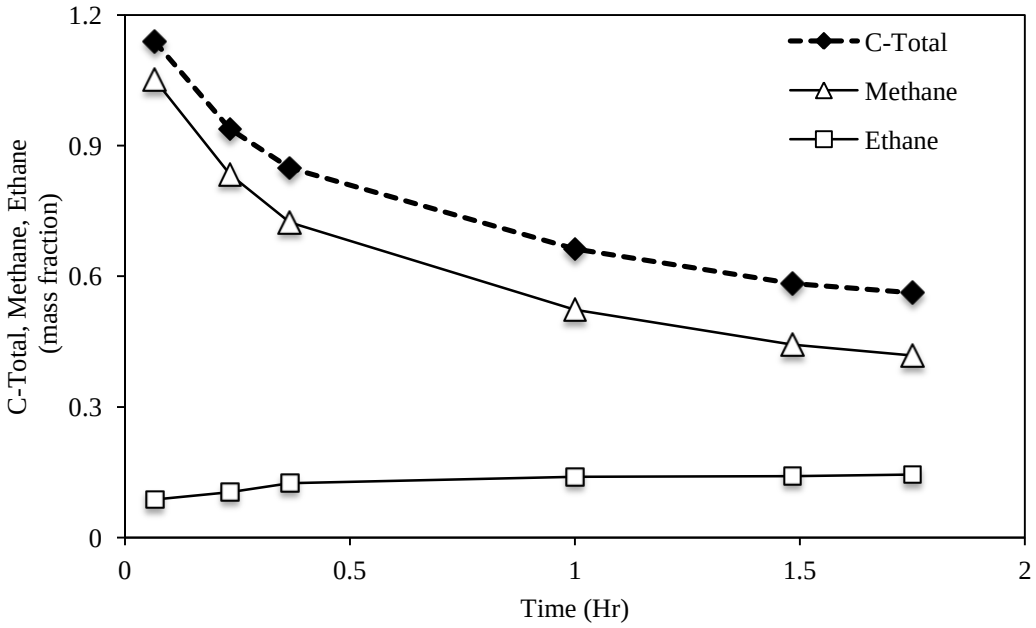


(B)

**Figure 3.5.4.a** $CH_4$ Degradation with Pd/Mg (3 g Mg with 0.06 wt% Pd) at pH 7. $[CH_4]_0$ = 0.207 □moles. (A) Degradation and byproducts; (B) Carbon mass recovery

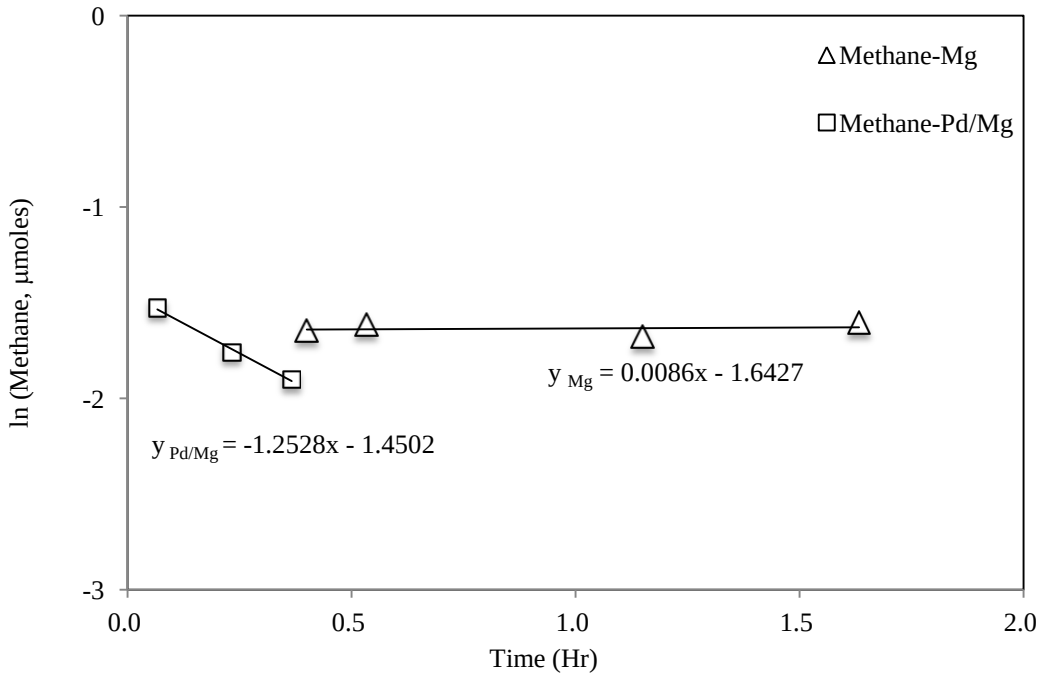


**Figure 3.5.4.b** Degradation kinetics $CH_4$ degradation with Pd/Mg (3 g Mg with 0.06 wt% Pd) at pH 7. $[CH_4]_0 = 0.207$ □moles.

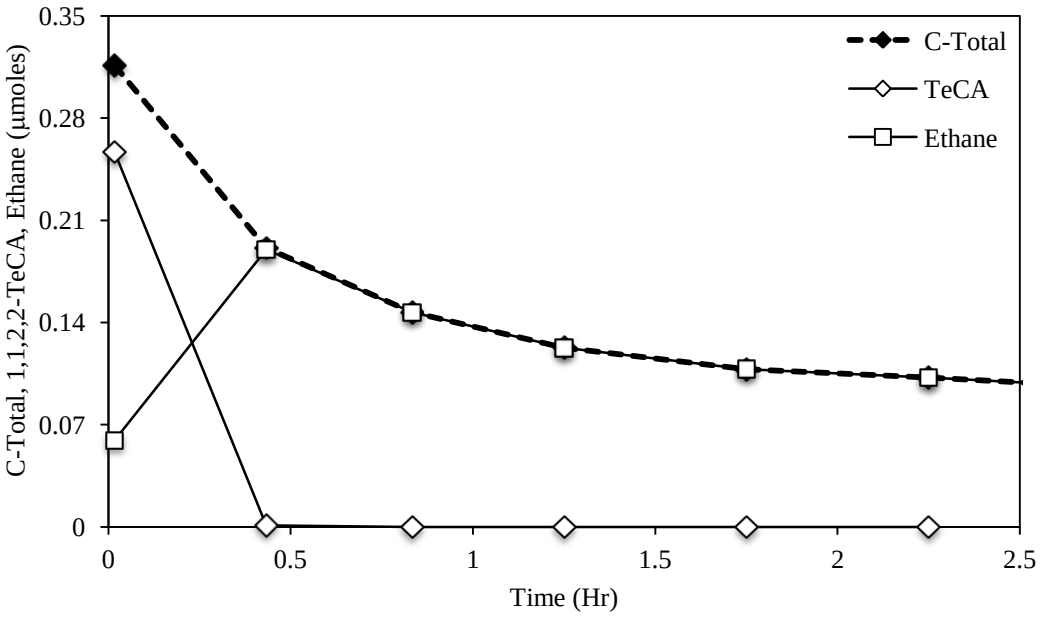


(A)

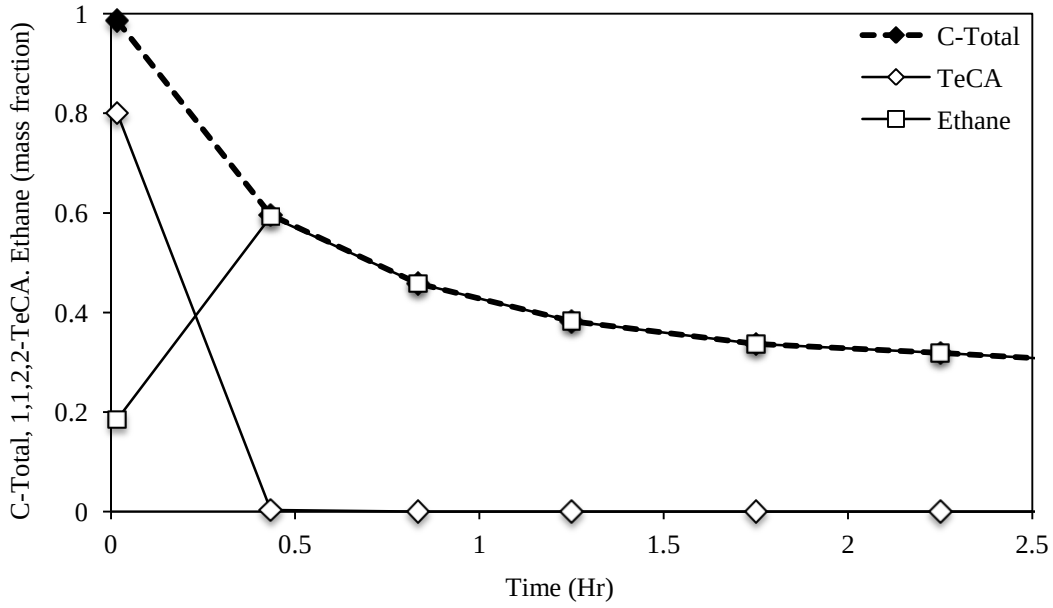


(B)

**Figure 3.6.1.a** 1,1,2,2-TeCA degradation with Pd/Mg (3 g Mg with 0.06 wt% Pd) at pH 7. $[1,1,2,2\text{-TeCA}]_0$ = 2.47 mM (200µl 198.75 mg/L 1,1,2,2-TeCA stock solution). (A) Degradation and byproducts; (B) Carbon mass recovery

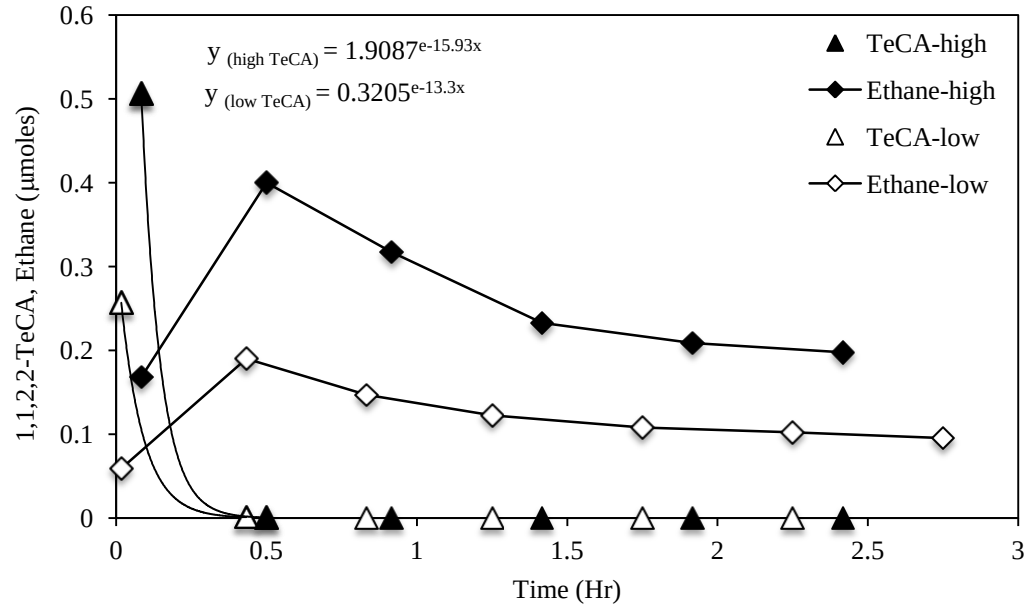


(A)

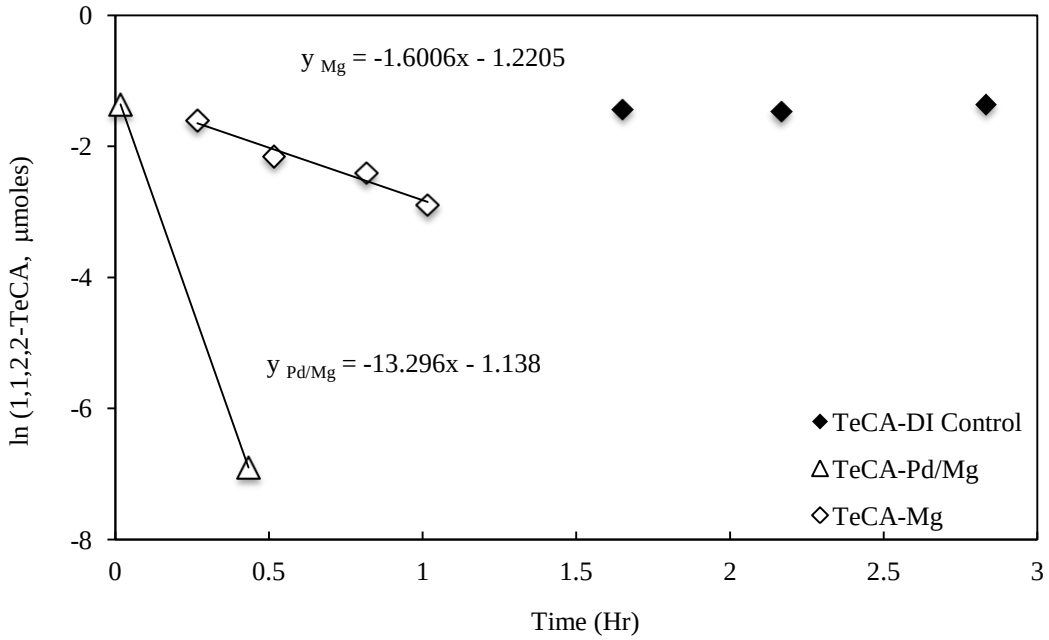


(B)

**Figure 3.6.1.b** Variable initial concentrations of 1,1,2,2-TeCA degradation with Pd/Mg (3 g Mg with 0.06 wt% Pd) at pH 7. High $TeCA_{[1,1,2,2\text{-}TeCA]0}$ = 6.17 mM (500µl 198.75 mg/L 1,1,2,2-TeCA stock solution); Low $TeCA_{[1,1,2,2\text{-}TeCA]0}$ = 2.47 mM (200µl 198.75 mg/L 1,1,2,2-TeCA stock solution); (A) Degradation process; (B) Degradation kinetics

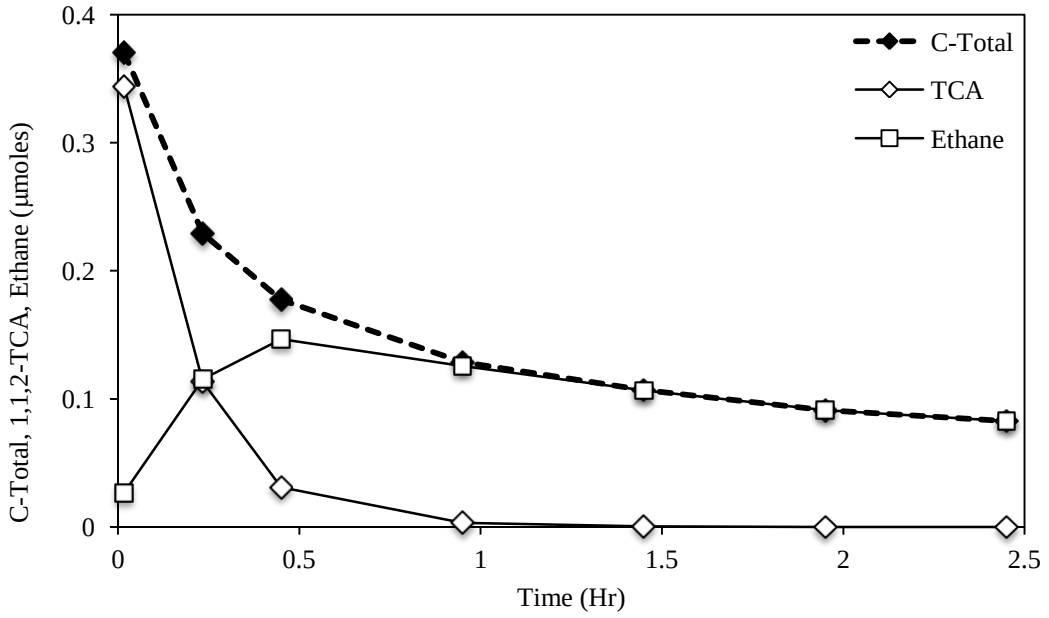


(A)

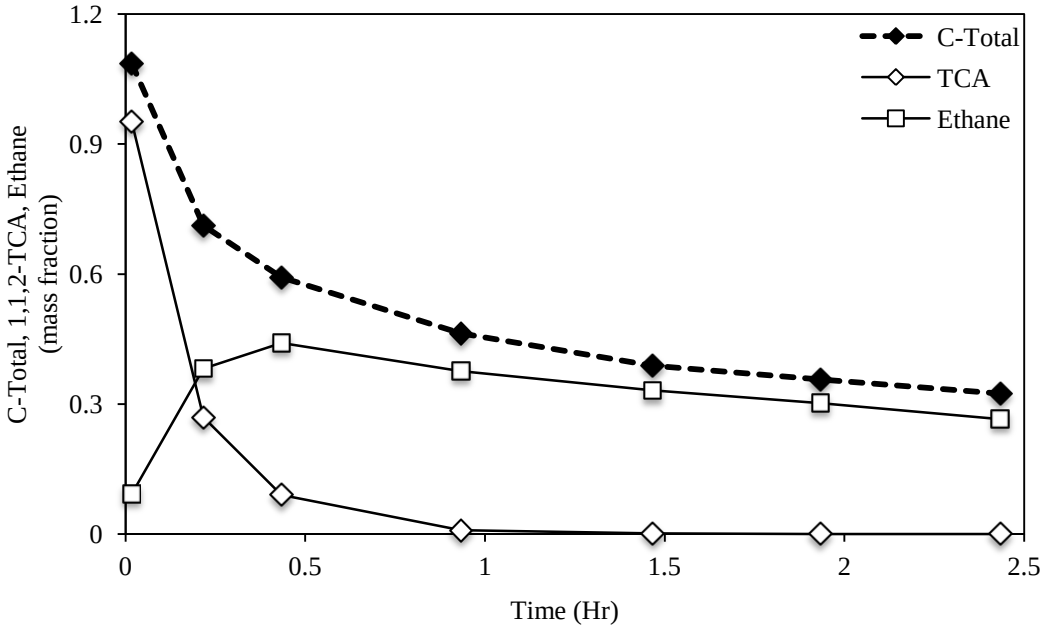


(B)

**Figure 3.6.2.a** 1,1,2-TCA Degradation with Pd/Mg (3 g Mg with 0.06 wt% Pd) at pH 7. $[1,1,2\text{-TCA}]_0$ = 2.80 mM (200µl 179.38 mg/L 1,1,2-TCA stock solution). (A) Degradation and byproducts; (B) Carbon mass recovery

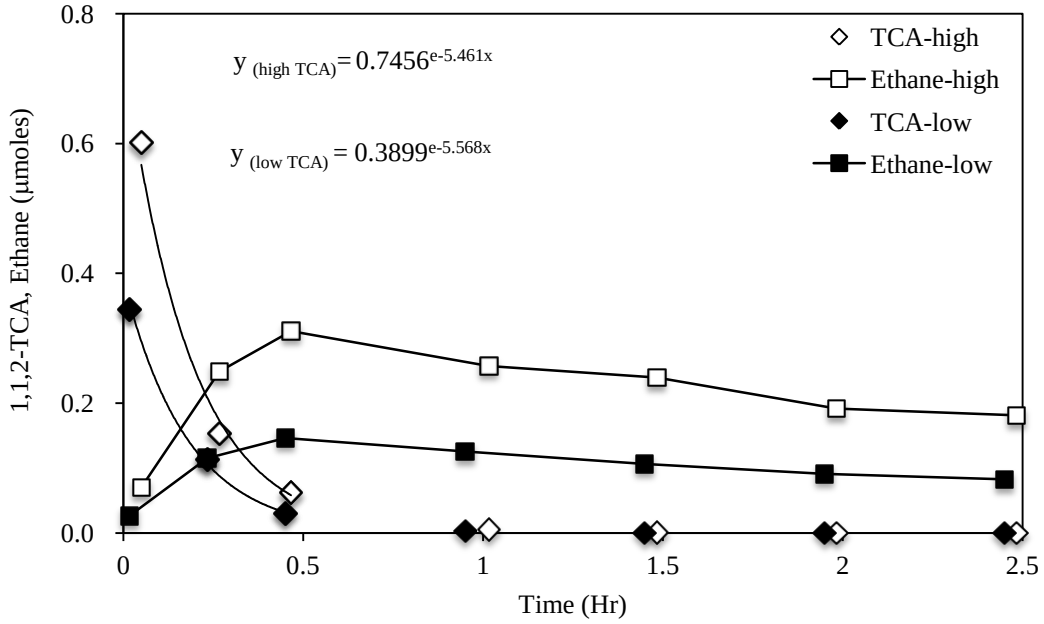


(A)

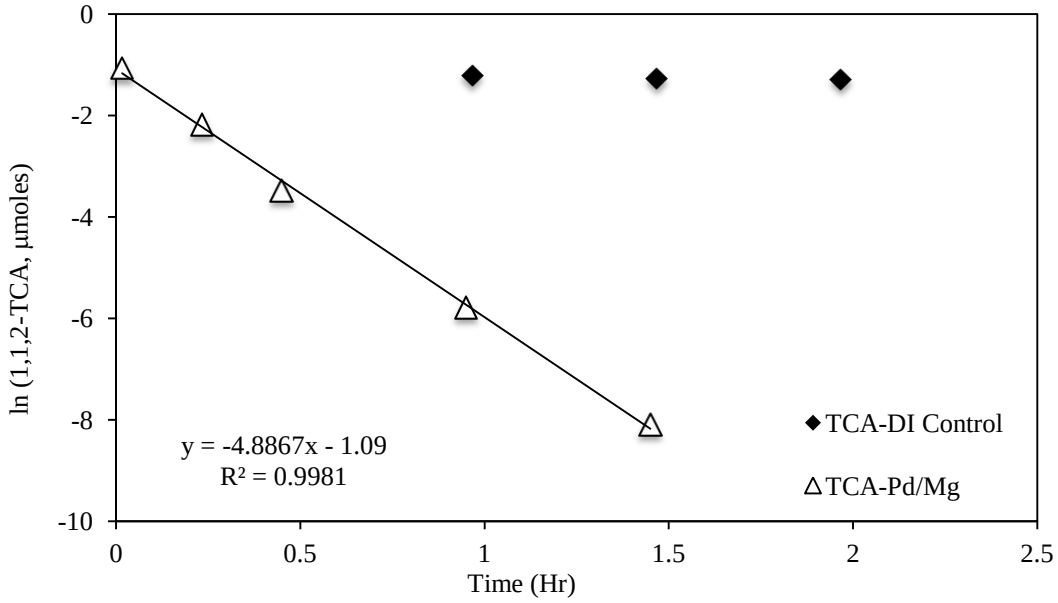


(B)

**Figure 3.6.2.b** Variable initial concentrations of 1,1,2-TCA degradation with Pd/Mg (3 g Mg with 0.06 wt% Pd) at pH 7. High $TCA_{[1,1,2\text{-}TCA]0}$ = 7.01 mM (500µl 179.38 mg/L 1,1,2-TCA stock solution); Low $TCA_{[1,1,2\text{-}TCA]0}$ = 2.80 mM (200µl 179.38 mg/L 1,1,2-TCA stock solution); (A) Degradation process; (B) Degradation kinetics

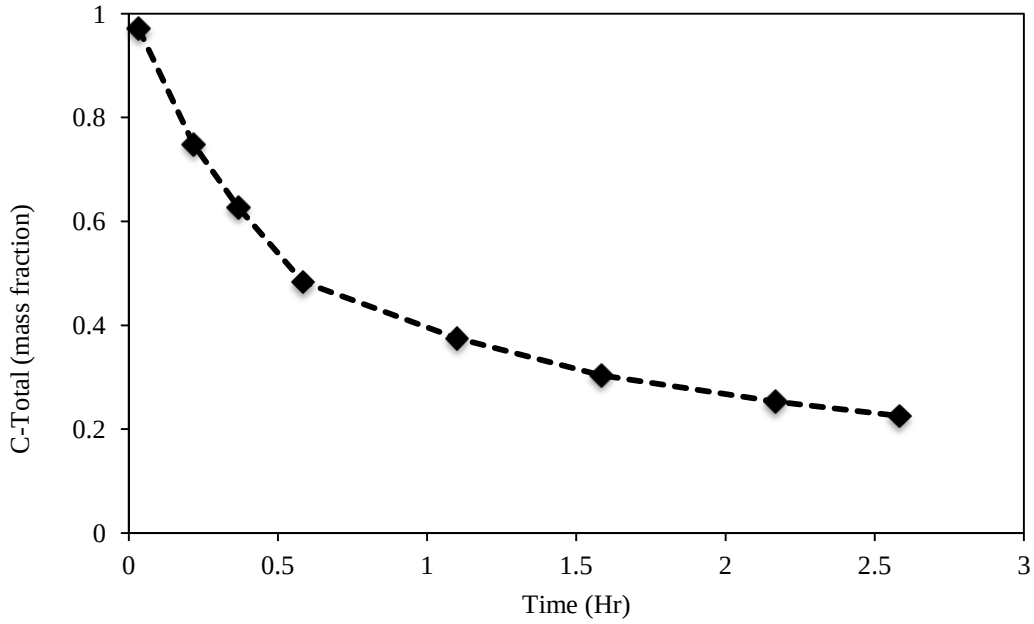


(A)

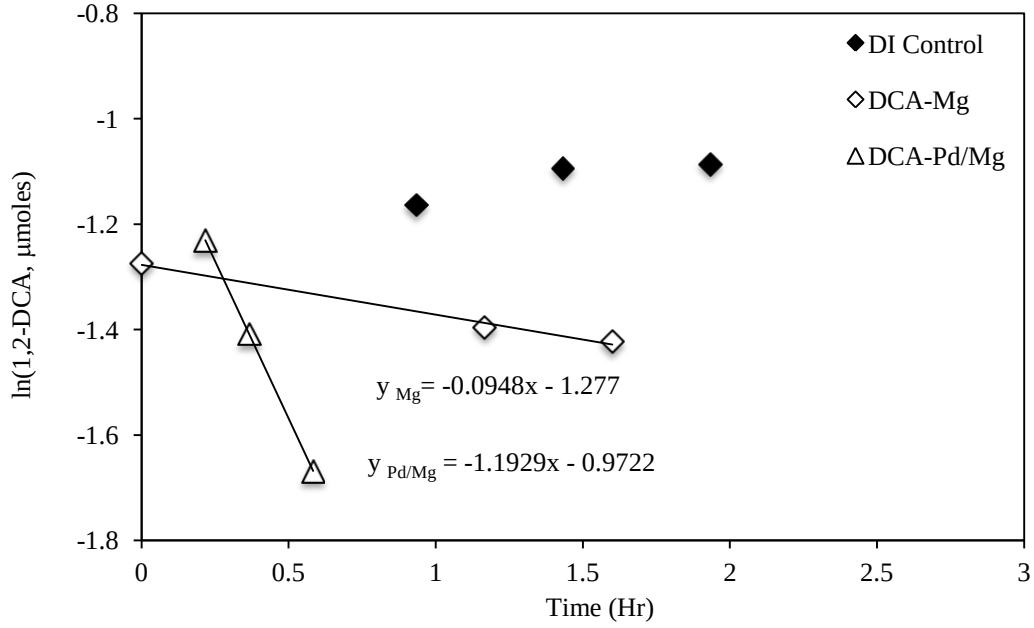


(B)

**Figure 3.6.3.a** 1,2-DCA Degradation with Pd/Mg (3 g Mg with 0.06 wt% Pd) at pH 7. $[1,2\text{-DCA}]_0$ = 3.29 mM (200µl 156.63 mg/L 1,2-DCA stock solution). (A) Carbon mass recovery; (B) Degradation kinetics

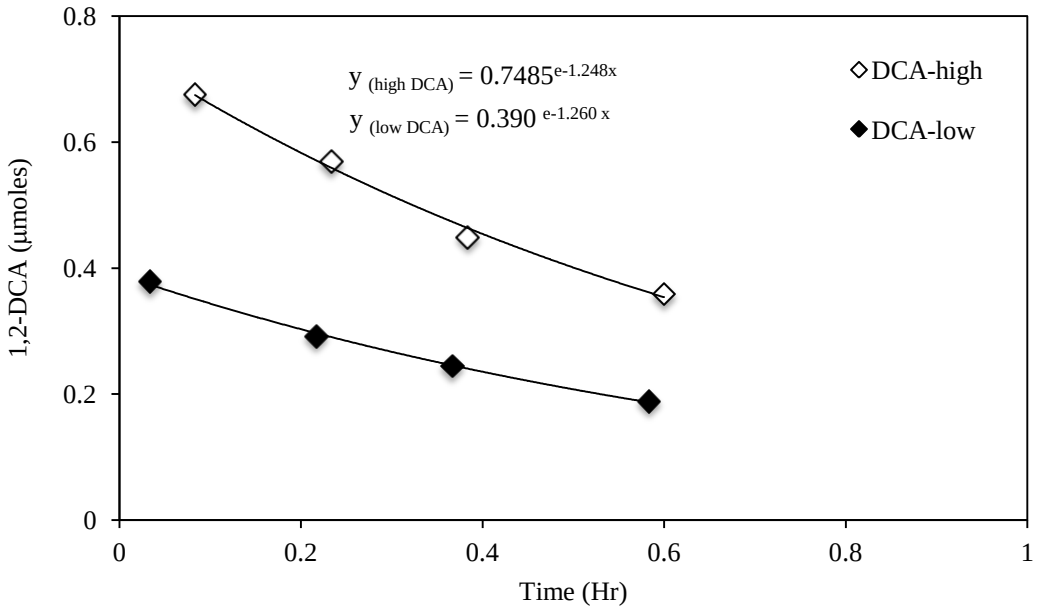


**Figure 3.6.3.b** Variable initial concentrations of 1,2-DCA Degradation with Pd/Mg (3 g Mg with 0.06 wt% Pd) at pH 7. $[\text{High-1,2-DCA}]_0$ = 8.23 mM (500µl 156.63 mg/L 1,2-DCA stock solution); $[\text{Low-1,2-DCA}]_0$ = 3.29 mM (200µl 156.63 mg/L 1,2-DCA stock solution)

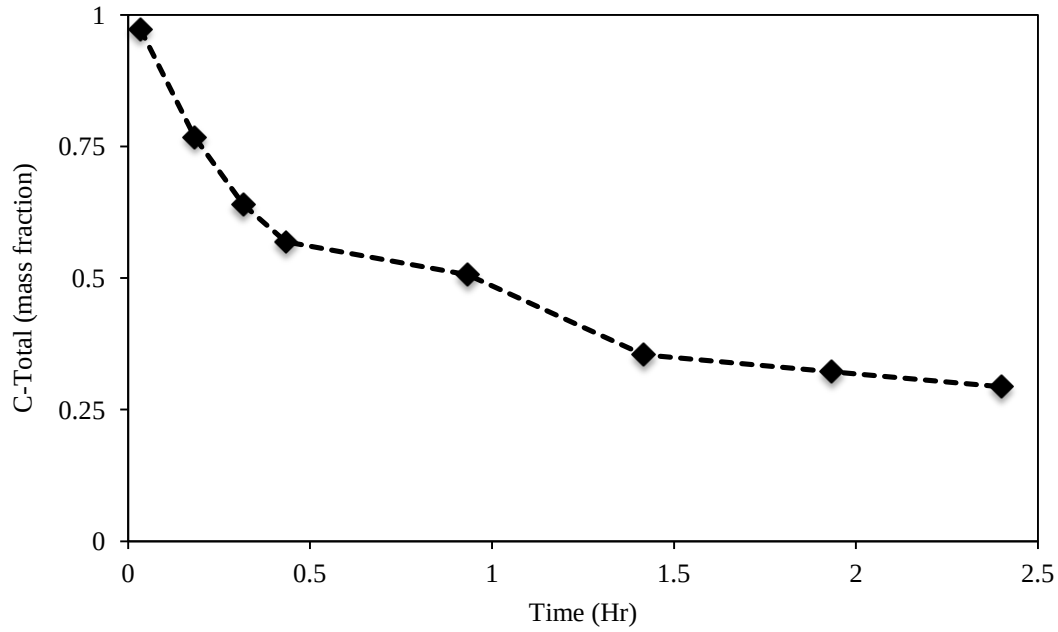


(A)

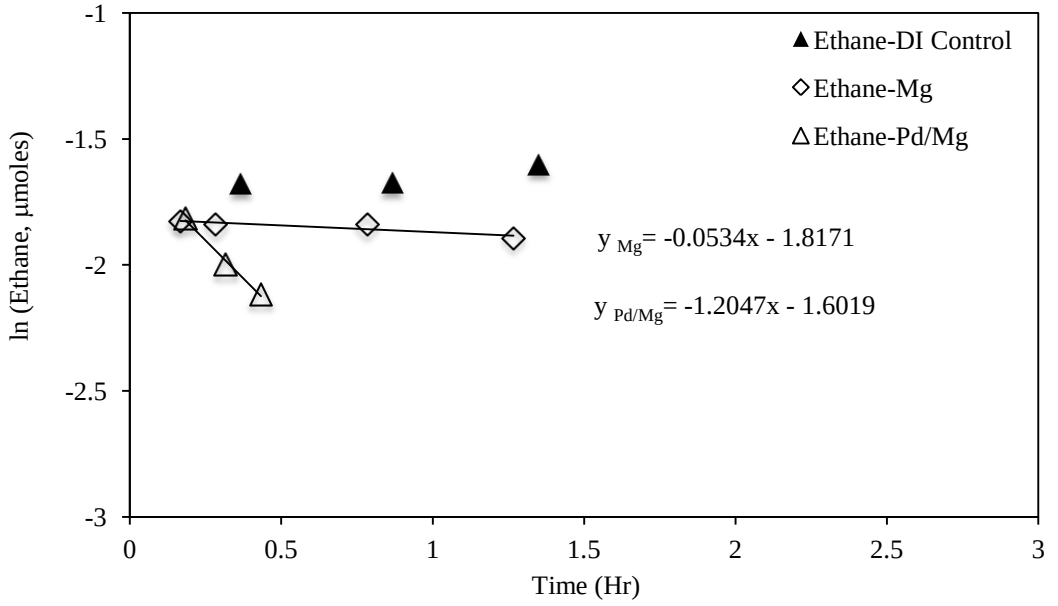


(B)

**Figure 3.6.4** Ethane degradation with Pd/Mg (3 g Mg with 0.06 wt% Pd) at pH 7. $[C_2H_6]_0$ = 0.207 µmoles. (A) Carbon mass recovery; (B) Degradation kinetics

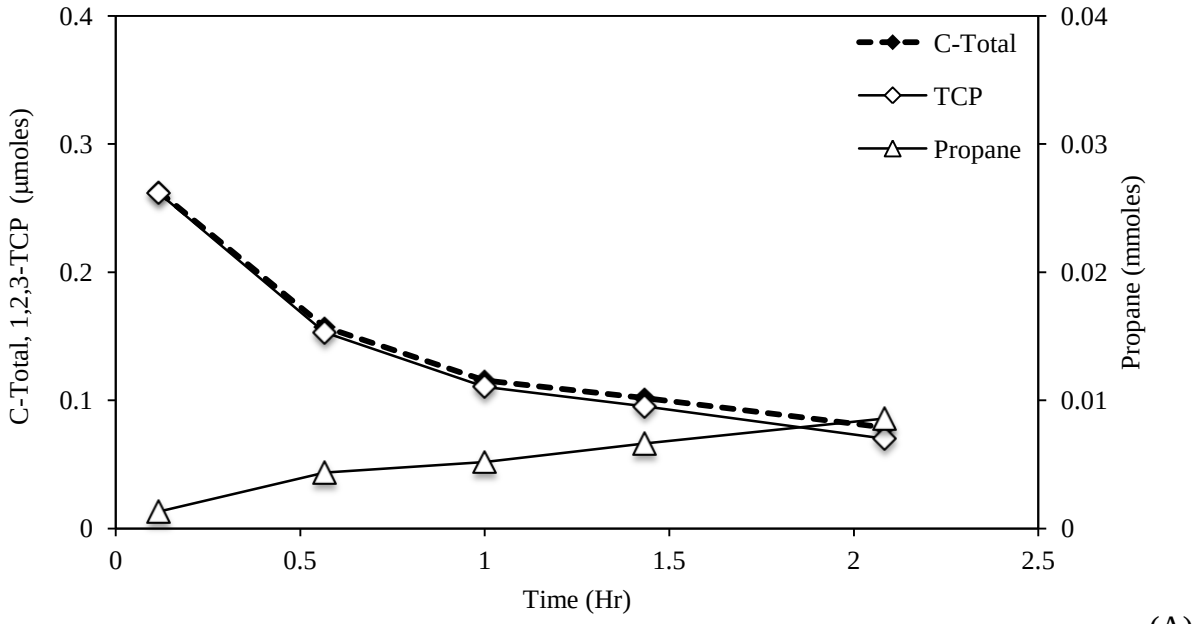


(A)

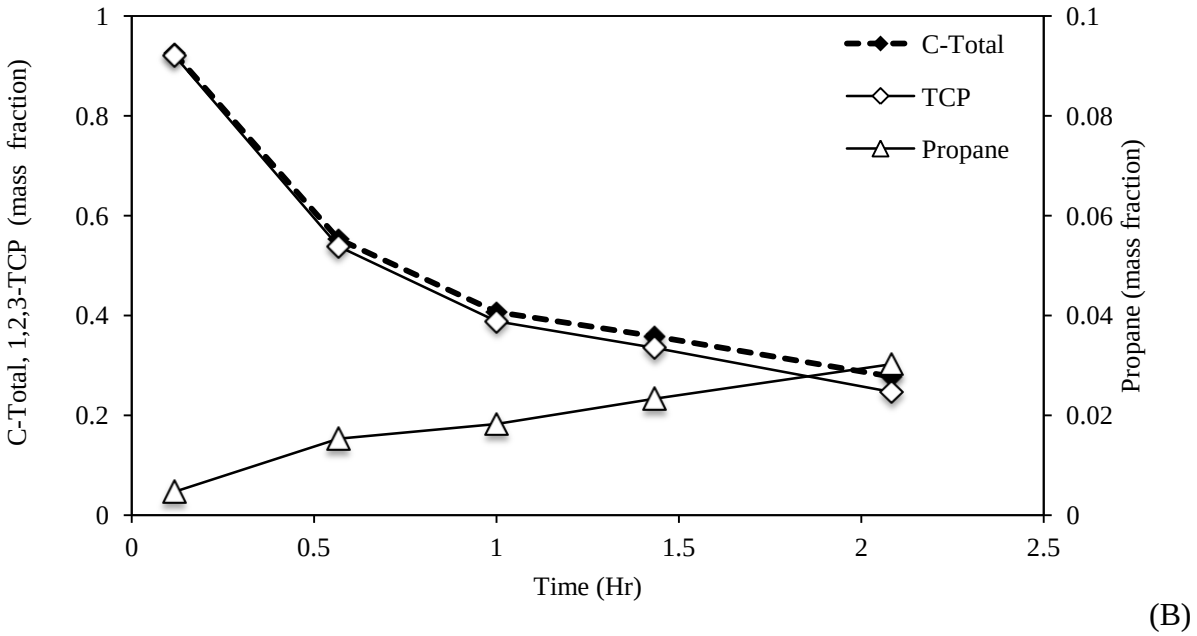


(B)

**Figure 3.7.1.a** 1,2,3-TCP degradation with Pd/Mg (3 g Mg with 0.06 wt% Pd) at pH 7. $[1,2,3\text{-TCP}]_0$ = 2.44 mM (200µl 172.5 mg/L 1,2,3-TCP stock solution). (A) Degradation and byproducts; (B) Carbon mass recovery

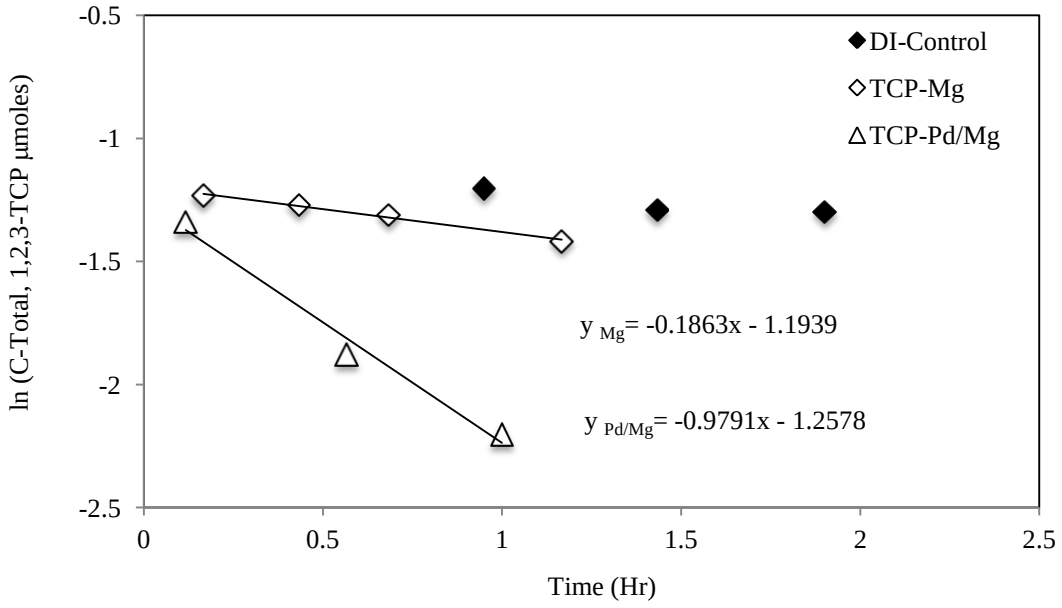


(B)

**Figure 3.7.1.b** Degradation kinetics of 1,2,3-TCP degradation with Pd/Mg (3 g Mg with 0.06 wt% Pd) at pH 7. $[1,2,3\text{-TCP}]_0$ = 2.44 mM (200µl 172.5 mg/L 1,2,3-TCP stock solution)

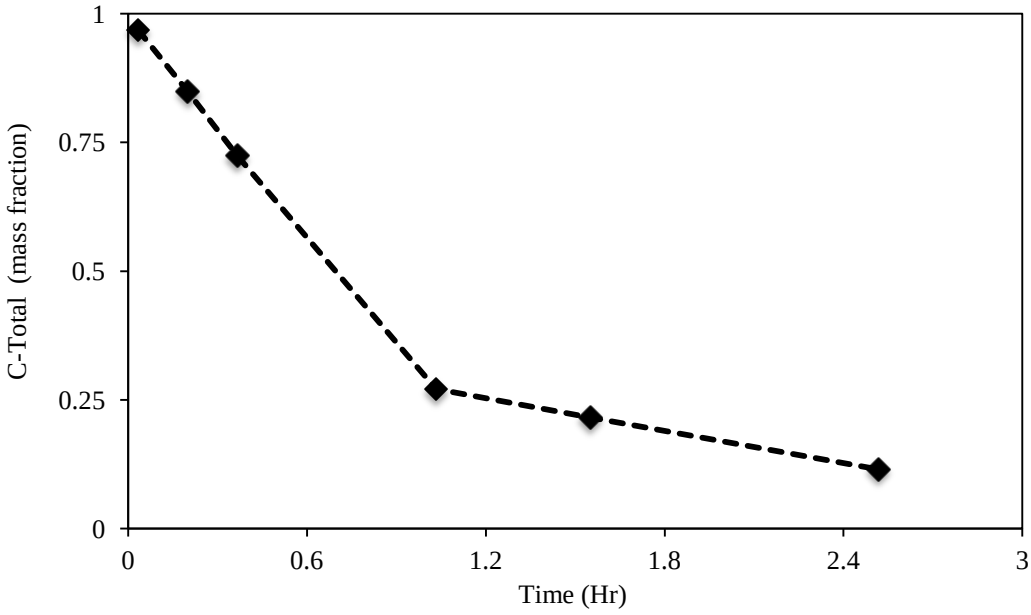


(A)

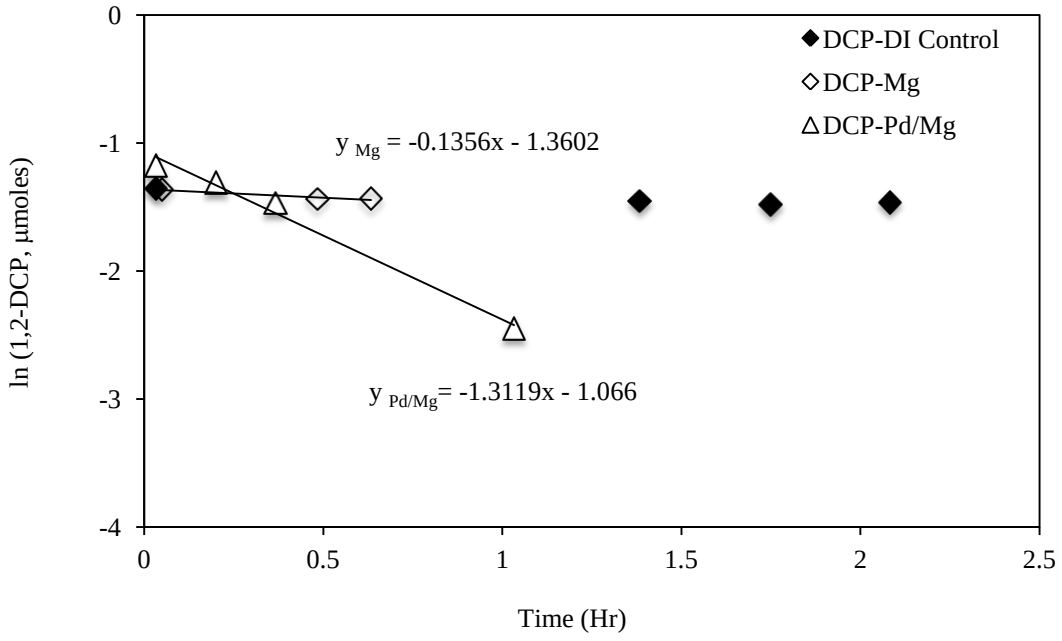


(B)

**Figure 3.7.2** 1,2-DCP degradation with Pd/Mg (3 g Mg with 0.06 wt% Pd) at pH 7. $[1,2\text{-DCP}]_0$ = 2.67 mM (200µl 144.5 mg/L 1,2-DCP stock solution). (A) Carbon mass recovery; (B) Degradation kinetics

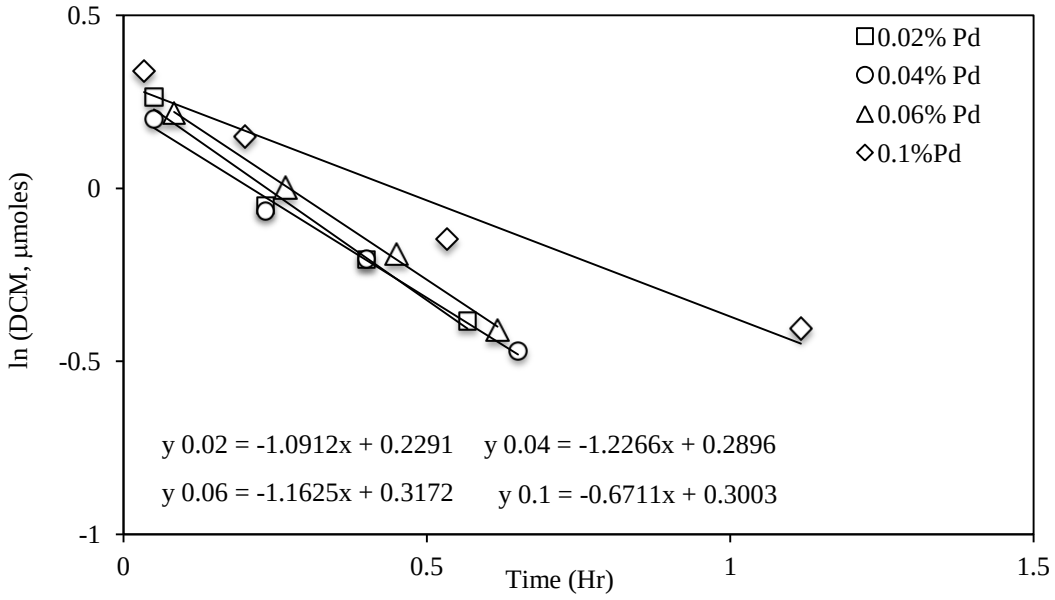


(A)

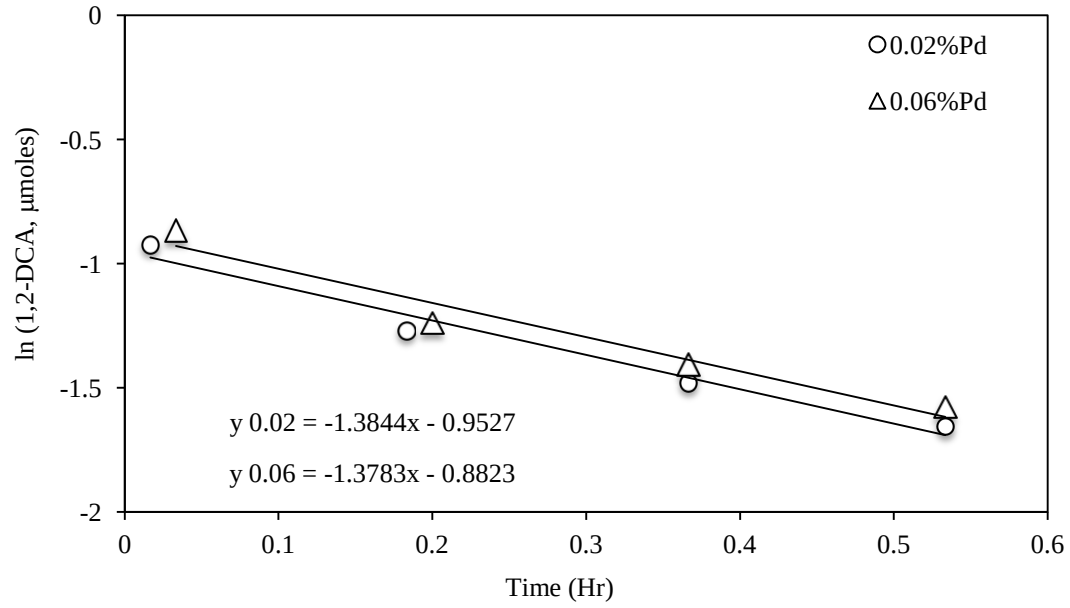


(B)

**Figure 3.8.1** Effect of Pd loading on CHC degradation kinetic with Pd/Mg (Mg fixed at 3 grams, Pd loading varied from 0.02 to 0.06 wt%). (A) Degradation kinetics of DCM degradation, $[DCM]_0$=10.20mM; (B) Degradation kinetics of 1,2-DCA degradation, $[1,2\text{-}DCA]_0$=3.09mM

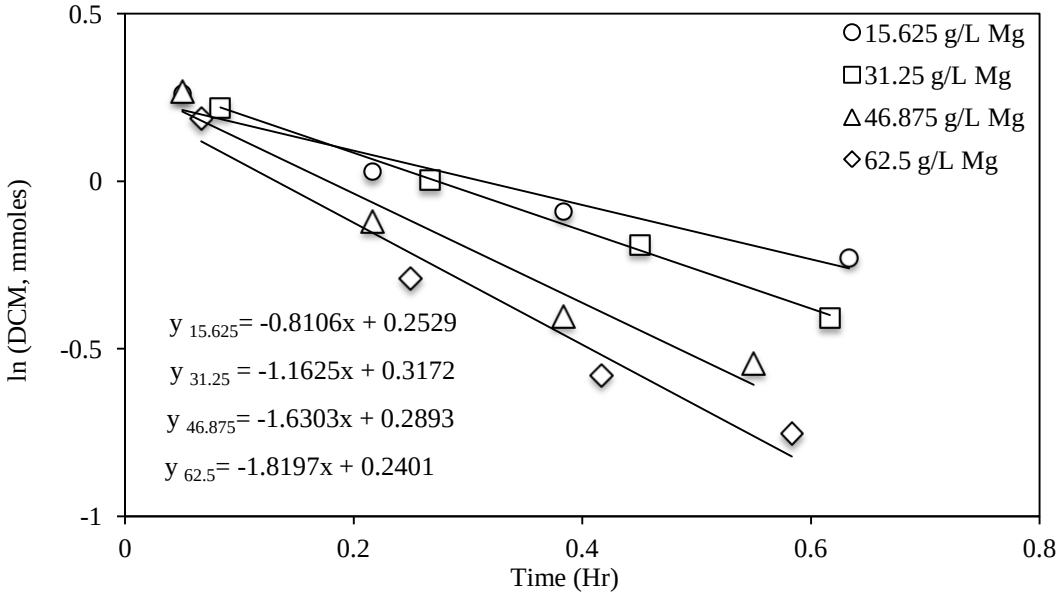


(A)

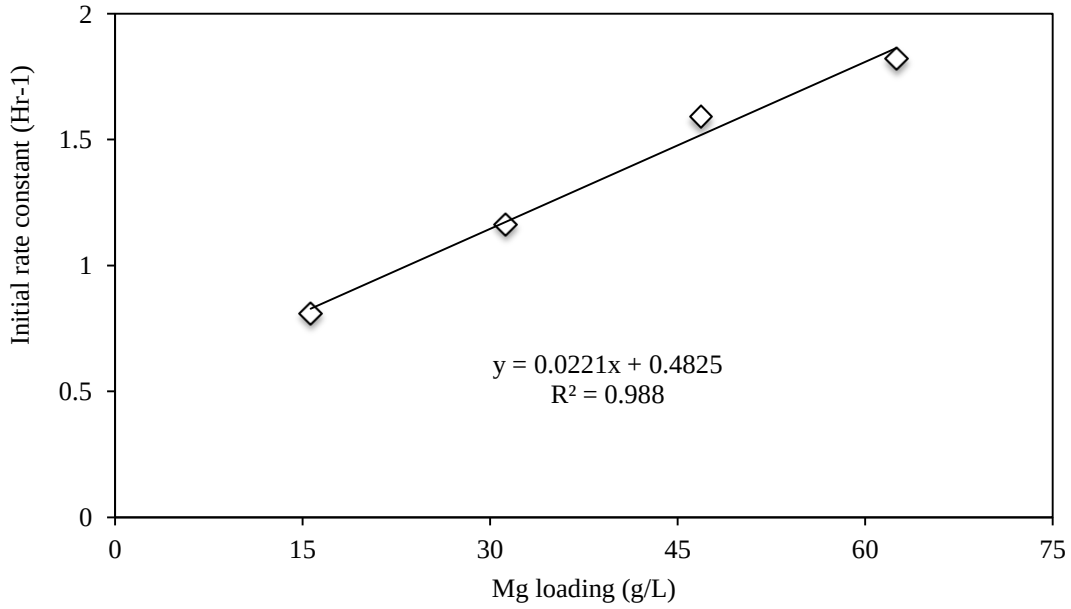


(B)

**Figure 3.9.1** Effect of Mg loading on DCM degradation kinetic with Pd/Mg (Pd fixed at 0.06 wt% of 3g Mg, Mg loading ranged from 15.625 to 62.5 g/L). $[DCM]_0$= 10.20 mM. (A) Degradation kinetics; (B) Linear relationship between initial degradation rate constant and Mg loading

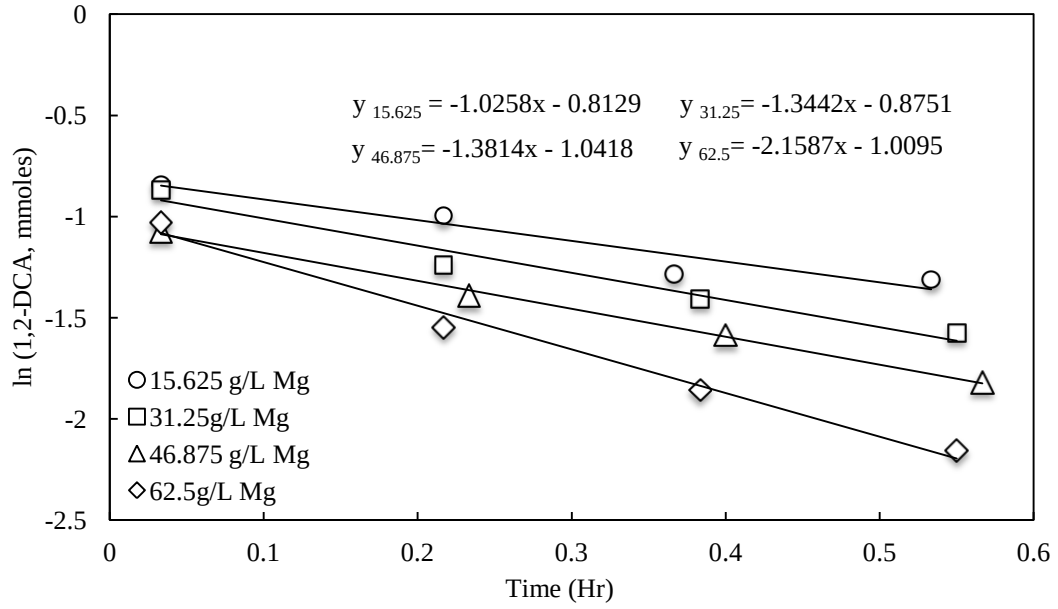


(A)

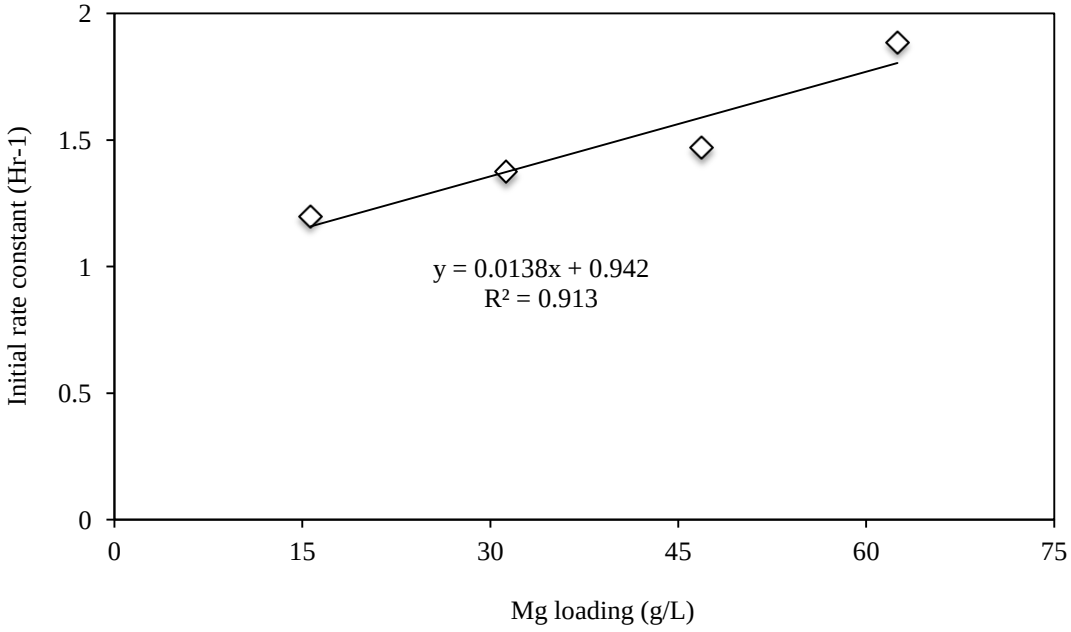


(B)

**Figure 3.9.2** Effect of Mg loading on 1,2-DCA degradation kinetic with Pd/Mg (Pd fixed at 0.06 wt% of 3g Mg, Mg loading ranged from 15.625 to 62.5 g/L). $[1,2\text{-DCA}]_0$= 3.09 mM. (A) Degradation kinetics; (B) Linear relationship between initial degradation rate constant and Mg loading

**Table 3.1** Pseudo first-order CHC degradation rate constant ($k_{obs,\ CHC}$, $h^{-1}$) with ZVM and Pd/Mg, corresponding coefficient of determination ($r^2$); and carbon mass recovery

| | Initial CHC[b] | | | | | | | |
|---|---|---|---|---|---|---|---|---|
| | | | CHC degradation with ZVM[c] | | | CHC degradation with Pd/Mg | | |
| CHC[a] | [Aqueous] (µg $liter^{-1}$) | Amount (µmol) | $k_{obs}$ | $r^2$ | *Mass balance* | $k_{obs}$ | $r^2$ | *Mass balance* |
| CT | 412 | 0.257 | 0.090 | 0.999 | 0.86 | 146 | 1.00 | 0.46 |
| CF | 385 | 0.30 | 0.065 | 0.981 | 0.82 | 46.2 | 1.00 | 0.40 |
| DCM | 866 | 0.98 | 0.050 | 0.913 | 0.78 | 1.16 | 0.998 | 0.28 |
| 1,1,2,2-TeCA-L[d] | 414 | 0.24 | --- | --- | --- | 13.3 | 1.00 | 0.32 |
| 1,1,2,2-TeCA-H[e] | 1035 | 0.60 | --- | --- | --- | 15.9 | 1.00 | 0.32 |
| 1,1,2-TCA-L[d] | 374 | 0.27 | 0.033 | 0.944 | 1.00 | 4.88 | 0.998 | 0.32 |
| 1,1,2-TCA-H[e] | 935 | 0.68 | --- | --- | --- | 5.46 | 0.992 | 0.27 |
| 1,2-DCA-L[d] | 326 | 0.32 | 0.033 | 0.791 | 0.94 | 1.26 | 0.998 | 0.23 |
| 1,2-DCA-H[e] | 815 | 0.88 | --- | --- | --- | 1.25 | 0.993 | 0.17 |
| 1,2,3-TCP | 359 | 0.23 | 0.102 | 0.985 | 0.90 | 0.989 | 0.983 | 0.30 |
| 1,2-DCP | 301 | 0.26 | 0.144 | 0.923 | 0.74 | 1.31 | 0.988 | 0.11 |

[a] – CHC– chlorinated hydrocarbon.

[b] – Additions based on calculated.

[c] – ZVM– zero-valent magnesium.

[d] – L– low initial concentration injected.

[e] – H– high initial concentration injected.

**Table 3.2** Pseudo first-order CHC degradation rate constant ($k_{obs,\ CHC}$, $h^{-1}$) at different initial pH values, corresponding coefficient of determination ($r^2$); and carbon mass recovery

| | CT degradation with ZVM[a] | | DCM degradation with ZVM[a] | |
|---|---|---|---|---|
| Initial pH | $k_{obs\text{-}1}$[b] | $r^2$ | $k_{obs\text{-}1}$[c] | $r^2$ |
| 4.5 | --- | --- | 0.519 | 0.984 |
| 5.0 | 0.226 | 0.984 | 0.253 | 0.996 |
| 5.5 | 0.193 | 0.996 | 0.190 | 0.983 |
| 6.0 | 0.172 | 0.949 | 0.161 | 0.965 |
| 6.5 | --- | --- | 0.124 | 0.988 |
| 7.0 | 0.145 | 0.963 | 0.050 | 0.913 |
| 8.0 | 0.123 | 0.837 | --- | --- |

[a] – ZVM– zero-valent magnesium.

[b] – $k_{obs\text{-}1}$– initial degradation rate constant of CT degradation, obtained from the equation that described the first-decay reaction within 1.5 hours

[c] – $k_{obs\text{-}1}$– initial degradation rate constant of DCM degradation, obtained from the equation that described the first-decay reaction within 3.0 h

# APPENDIX A ANALYSIS AND CALCULATIONS

## A.1 CALCULATIONS FOR DETERMINING AQUEOUS CONCENTRATIONS AND MASS OF VOLATILES IN REACTORS (ADAPTED FROM POWELL AND AGRAWAL 2011)

### A.1.1 **Methane**

Concentration of $CH_4$ within the reactor when establishing the calibration curve will be calculated as follows:

1. The number of moles of gaseous $CH_4$, *n*, injected by syringe into the liquid phase, was determined using the ideal gas law:
   a. $n = \frac{PV}{RT}$

      where *P* = Pressure, 1 atm; *V* = volume of gas injected , L;

      R= gas constant , 0.0821 atm liter mole$^{-1}$ K$^{-1}$; *T* = temperature, 298 K;

2. The total mass (*m*) of $CH_4$ in mg in the aqueous phase was calculated by:

   A.1.2 $m = n * FW * 1000$

      where $FW$ = formula weight of methane, 16 g mole$^{-1}$; 1000 = conversion factor

3. Find the water partitioning coefficient ($f_w$)
   a. $f_w = \frac{1}{(1+k'_H(\frac{V_a}{V_w}))}$

where $k'_H$ = Henry's Constant for methane ($C_{air}/C_{water}$) at 20°C, 28.5 [D] (Schwarzenbach *et al.* 1995); $V_a$ = volume of head space; $V_w$ = volume of liquid

The $CH_4$ mass in the aqueous phase ($m_w$) and in gas phase ($m_a$) after partitioning were calculated as:

b. $m_w = m * f_w$

c. $m_a = m * (1 - f_w)$

4. The concentration of $CH_4$ in aqueous phase ($C_w$) and headspace ($C_a$) were determined as:

   a. $C_w = \frac{m_w}{V_w}$

   b. $C_a = \frac{m_a}{V_a}$

5. Plot a standard curve with peak areas on the x-axis and $C_a$ on the y-axis

   a. Determine $C_a$ in the reactor sample by plugging the peak area into the best fit line equation (y = mx, where peak area is x).

### A.1.2 **Chlorinated hydrocarbon**

1. CHC stock solutions were prepared by adding a known amount of pure compound to a 160 mL glass serum bottle filled completely with Milli-Q water. Seal bottle with Teflon lined rubber septa and aluminum crimp. Rotate bottle, end-over-end at 30 rpm for at least 48 hours to allow compound to completely dissolve (Burris *et al.* 1996).
2. The concentration of CHC stock solution ($C_s$), in mg liter$^{-1}$, was determined as:

   a. $m_t = \rho_{CHC} * V_{pure}$

where $\rho_{CHC}$ = density of CHC, g/cc; $V_{pure}$ = volume of pure CHC added by gas tight syringe

b. $C_s = m_t * V_w$

where $V_w$ = volume of water, liter

3. Extract CHC stock solution with gas-tight, glass syringe and add to the reactors.
4. Calculate the concentration ($C_t$), in µmol liter$^{-1}$, and total mass ($m_t$), in µg, of CAH in the reactor before partitioning

a. $C_t = \frac{V_{stock} * C_s}{V_w * (FW)}$

where $V_{stock}$ = volume of stock solution added, µL; $V_w$ = volume of liquid in the reactor, mL; $FW$ = formula weight of CHC, g mol$^{-1}$

b. $m_t = C_t * V_w$

5. A dimensionless constant of CHC at 20°C was used to determine the fraction of CHC concentration after equilibration between the gas and liquid phases:

a. $f_w = \frac{1}{(1+k'_H(\frac{V_a}{V_w}))}$

where $k'_H$ = dimensionless Henry's Constant for CHC ($C_{air}/C_{water}$) at 20°C, [D]; $V_a$ = volume of head space; $V_w$ = volume of liquid in the reactor

6. Determine the mass in aqueous phase ($m_w$) and mass in head space ($m_a$), in µg

a. $m_w = m_t * f_w$

b. $m_a = m_t * (1 - f_w)$

7. Convert the mass in aqueous phase to aqueous concentration ($C_w$), µg liter$^{-1}$, and mass in head space to concentration in air ($C_a$), µg liter$^{-1}$

a. $C_w = \frac{m_w}{V_w}$

b. $C_a = \frac{m_a}{V_a}$

8. The pseudo first-order degradation rate constant, $k_{obs}$; $h^{-1}$, was determined from the slope of ln [CHC amount, umol] versus time, Hr, scatter plots for the first 4 points

**Table A1** Properties and purity of CHCs evaluated in this work

| | | | Values computed at 20 $^{o}$C | | |
|---|---|---|---|---|---|
| CHC[a] | Chemical name | Provider | Density (g/cm$^3$) | Henry's constant [D][b] | Purity (%) |
| CT | Carbon tetrachloride | Fisher Scientific | 1.587 | 0.547 | 99.0 |
| CF | Chloroform | Fisher Scientific | 1.472 | 0.122 | 99.8 |
| DCM | Dichloromethane | Fisher Scientific | 1.325 | 0.0745 | 99.9 |
| 1,1,2,2-TeCA | 1,1,2,2-Tetrachloroethane | Arcos Organics | 1.590 | 0.0141 | 98.0 |
| 1,1,2-TCA | 1,1,2-Trichloroethane | Alpha Chemicals | 1.435 | 0.0287 | 98.0 |
| 1,2-DCA | 1,2-Dichloroethane | Sigma-Aldrich | 1.256 | 0.0318 | 99.0 |
| 1,2,3-TCP | 1,2,3-Trichloropropane | Arcos Organics | 1.380 | 0.009 | 98.0 |
| 1,2-DCP | 1,2-Dichloropropane | Arcos Organics | 1.156 | 0.0907 | 98.0 |

[a]- CHC – chlorinated hydrocarbon

[b]- Dimensionless Henry's constants were obtained from USEPA (2012).

### A.1.3 **References**

Burris, D. R.; Delcomyn, C. A.; Smith, M. H.; Roberts, A. L. Reductive dechlorination of tetrachloroethylene and trichloroethylene catalyzed by vitamin B-12 in homogeneous and heterogeneous systems. *Environ. Sci. and Technol*. ***1996***, *30* (10), 3047−3052.

Powell, C. L.; Agrawal, A. Biodegradation of trichloroethene by methane oxidizers naturally associated with wetland plant roots. *Wetlands* **2011**, *31* (1), 45−52.

Schwarzenbach, R. P.; Gschwend, P. M.; Imboden, D. M. *Environmental organic chemistry illustrative examples, problems, and case studies*. John Wiley and Sons, Inc.: New York, 1995; p. 392.